Research Square

Preprints are preliminary reports that have not undergone peer review.
They should not be considered conclusive, used to inform clinical practice,
or referenced by the media as validated information.

Enhanced Ammonia Sensing By Cost-Effective ZnO Thin Films Through Yttrium Doping

K. Ravichandran (kkr1365@yahoo.com)
AVVM Sri Pushpam College (Autonomous), Poondi, Thanjavur 613503, Tamil Nadu, India
A. Jansi Santhosam
AVVM Sri Pushpam College (Autonomous), Poondi, Thanjavur 613503, Tamil Nadu, India
M. Aldossary Omar
King Saud University
Mohd Ubaidhulla
King Saud University

Research Article

Keywords: Thin films, Yttrium doped ZnO, Nebulizer Spray Pyrolysis, NH3 sensor

Posted Date: June 12th, 2021

DOI: https://doi.org/10.21203/rs.3.rs-607950/v1

License: This work is licensed under a Creative Commons Attribution 4.0 International License.
Read Full License

Full Length Article

Enhanced ammonia sensing by cost-effective ZnO thin films through Yttrium doping

K. Ravichandran[a,*] A. Jansi Santhosam[a,b] Omar M. Aldossary[c], Mohd Ubaidullah[d]

[a]*Materials Science Research Laboratory, PG and Research Department of Physics, AVVM Sri Pushpam College (Autonomous), (Affiliated to Bharathidasan University, Tiruchirappalli.) Poondi, Thanjavur-613 503, Tamil Nadu, India.*
[b] *Research Department of Physics, Kunthavai Naachiyaar Govt. Arts College for Women (Autonomous), (Affiliated to Bharathidasan University, Tiruchirappalli.)Thanjavur – 613 007, Tamil Nadu, India.*
[c]*Department of Physics and Astronomy, College of Science, King Saud University, P.O. Box 2455, Riyadh 11451, Saudi Arabia.*
[d]*Department of Chemistry, College of Science, King Saud University, Riyadh 11451, Saudi Arabia.*

Corresponding author:
Dr. K. Ravichandran,
Associate Professor of Physics,
PG and Research Department of Physics,
AVVM Sri Pushpam College (Autonomous),
Poondi, Thanjavur-613 503, Tamil Nadu, India.
E. mail: kkr1365@yahoo.com
kkravi1365@gmail.com

Graphical abstract

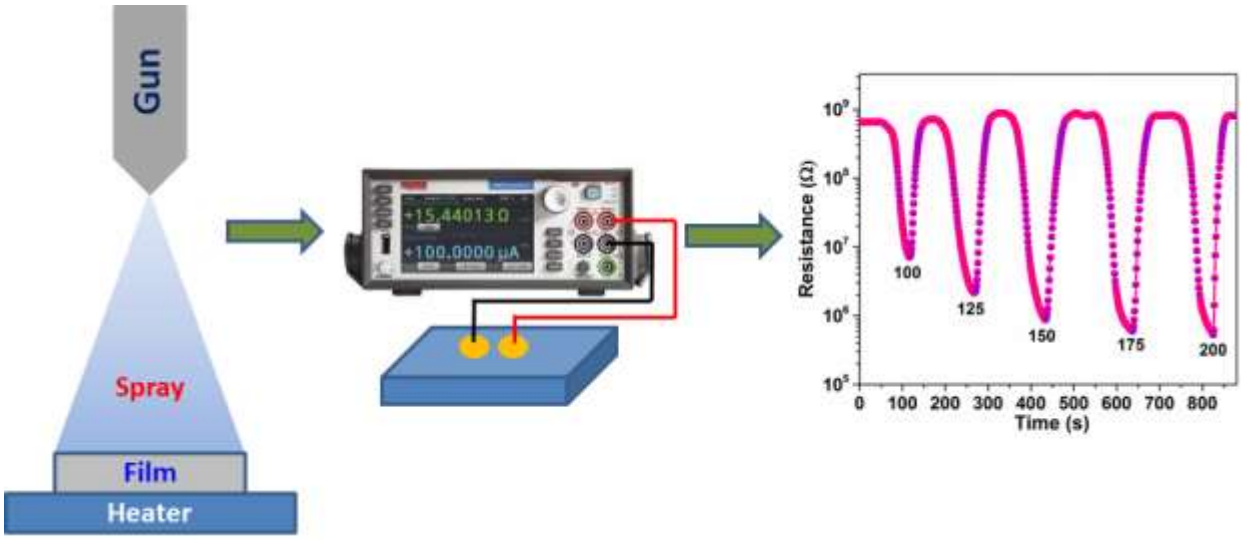

Nebulizer spray coated yttrium doped ZnO thin film for ammonia vapour sensing

Highlights

- Yttrium doped ZnO thin films have been fabricated for room temperature ammonia sensor
- Surface roughness and oxygen vacancies are created by yttrium doping
- Morphology and defect based gas sensing performance are explained
- The maximum sensitivity observed for 5% yttrium doped ZnO film
- The gas sensing mechanism yttrium doped ZnO film was proposed

Enhanced ammonia sensing by cost-effective ZnO thin films through Yttrium doping

Abstract

Yttrium (Y) doped (doping concentration - 0, 1, 3 and 5 wt%) ZnO thin films were deposited using spray pyrolysis technique. The structural, surface morphological, optical and compositional properties were analysed using X-Ray diffraction (XRD), Atomic Force Microscopy (AFM), UV-vis NIR spectrophotmetry (UV), photoluminescence study (PL) and elemental composition analysis. Ammonia vapour sensing properties such as response/recovery, stability and repeatability were studied at room temperature. XRD results confirmed that the prepared samples have hexagonal wurtzite structure. ZnO:Y thin film with 5 wt% yttrium doping exhibits excellent sensing response of 99, fast response/recovery times of 29 s/ 7 s which may be due to the existence of oxygen vacancies in the case of ZnO:Y (5 wt%) film sample confirmed by photoluminescence (PL) study. These oxygen vacancies attract more electrons and thus enhance the gas sensing. In addition, increase in the number of active sites caused by the substitution of Y^{3+}(trivalent) ions into the Zn^{2+} (divalent) regular sites as confirmed by the observed M-B (Moss-Burstein) effect also causes an enhancement in the gas sensing. Surface roughness, another reason for the enhanced sensitivity, has been confirmed by AFM.

Key words: *Thin films, Yttrium doped ZnO, Nebulizer Spray Pyrolysis, NH_3 sensor*

1. Introduction

Recent days, ammonia gas sensors play an important role in the industries of explosives, fertilizers, textiles and plastics [1]. The acceptable limit of ammonia for human body is 25 ppm, beyond which it can affect the various parts of the body causing damage to skin, eyes and respiratory tract [2]. Hence, researchers pay attention on making cost-effective ammonia sensors with improved '3S' parameters *viz.* sensitivity, stability and selectivity [3].

Plenty of metal oxide semiconductors like V_2O_5, SnO_2, TiO_2, NiO, $BaTiO_3$ and ZnO are widely used to detect ammonia vapours [4-10]. Of these, ZnO is one of the promising materials due to its attracting properties which include high thermal and chemical stability, non-toxicity, wide band gap, availability, environmentally benign nature, low-cost and ease of doping [11].

Moreover, literature survey shows that the gas sensing ability of ZnO can be improved through the addition of suitable dopants. Select dopants desirably alter the energy gap and surface morphology of the host material. In addition, doping causes an increase in defects and carrier concentration and thereby favouring the sensing phenomena [12]. Various rare earth metals like lanthanum, cerium, erbium, terbium, gadolinium and yttrium [13-18] have been used as dopants owing to their unique properties. Among the various rare earth elements,yttrium is used as dopant because of its peculiar properties arising from the 4f shell such as changes in energy band structure, morphology, surface to volume ratio and ability for creating more active centres at the grain boundaries [19, 20]. Thus, the gas sensing response of ZnO can be improved by the addition of suitable proportion of yttrium.

Li and co-workers reported that yttrium doped ZnO nanofibers exhibit good sensing to acetic acid [21] due to the large specific surface area and small grain size of ZnO:Y nanofibers. Nithya *et al*. reported that yttrium doped titania nanoparticles prepared towards ethanol sensing exhibit short response/recovery times and long-term stability that may be due to the small crystal size

and increase in oxygen vacancies [22]. Shruthi *et al*. reported that Y_2O_3-In_2O_3 nanocomposites exhibit sharp response/recovery times for methanol detection. It may be attributed to the formation of hetero junction between host and dopant materials [23]. However, to the best of our knowledge yttrium doped ZnO thin films towards ammonia sensing is scarcely available in the literature.

Undoped and doped ZnO films can be prepared by different techniques like magnetron sputtering, hydrothermal, sol gel, wet chemical route, SILAR and nebulizer spray Pyrolysis method [24-29]. Among these methods, nebulizer spray pyrolysis offers many advantages: economic, simple and safe, facilitate large surface area coating, flexible process parameters and uniform thickness [30].

In this work, undoped and yttrium doped ZnO film sensors have been developed using cost effective nebulizer spray pyrolysis method. The sensing ability, response and recovery times and stability of the sensor towards the reducing vapour (NH_3) at room temperature were studied and reported.

2. Experimental details

2.1 Chemicals used

Zinc acetate dihydrate ($Zn(CH_3COO)_2.2H_2O$), yttrium nitrate hexahydrate($Y(NO_3)_3 \cdot 6H_2O$) were purchased from Sigma Aldrich and used without any further purification.

2.2 Film deposition

$Zn(CH_3COO)_2.2H_2O$ and $Y(NO_3)_3 \cdot 6H_2O$ were used as host and dopant precursors, respectively and methanol (10 mL) was used as solvent. Four sets of stock solutions (0.2 M) were prepared with dopant concentrations 0, 1, 3 and 5wt%. The solution was stirred for 15 minutes at 35^oC. Substrates (glass) were cleaned well with usual cleaning procedure and then

placed on the substrate holder (hot plate) maintained at 450^{o}C. The solution was sprayed on the hot substrates over the area of 2.5 x 7.5 cm^{2}. The distance between the spray nozzle and substrate was optimized as 30 mm. Nebulizer was mounted with the help of a stand and slowly moved in horizontal direction to cover large surface area. After the deposition, the hot plate was allowed to cool to room temperature.

2.3 Characterization techniques

The structural characterization of the prepared thin films was made using X-ray diffraction (Panalytical X'Pert PRO) using Cu-K_{α} radiation (λ=0.1540nm). Stylus profilometer was used to measure the thickness of the prepared films. Atomic Force Microscope was used to analyse the surface topography of the samples. A UV-vis-near-IR spectrophotometer (Perkin Elmer Lamda-35) was used to study the transmittance. Fluorescence spectrophotometer (Perkin Elmer LS55) was used to record the photoluminescence spectra at room temperature (λ_{exc}= 325 nm). Keithley Meter model-2450 was used to study the room temperature (32^{o}C) ammonia sensing.

2.4 Sensing study

The gas sensing setup consists of a cylindrical chamber and a computer assisted Keithley electrometer (model- 2450). The prepared thin film was placed inside the chamber and to attain a baseline, the sample's resistance was measured under dry air. The ammonia taken in solution form was injected into the chamber with the help of microliter syringe. The introduction of NH_3 vapour produces a marked change in the resistance of the sensor. The reduction in resistance confirms the n-type behaviour of the sensor towards reducing vapours like NH_3. The change in resistance was observed using Keithley meter. The chamber is opened to air ambience when the resistance attained the saturation level. The resistance values were measured with respect to base line and recorded for different ammonia concentrations.

3.Results and discussion

3.1 XRD study

Figure 1 shows the X-Ray diffraction patternsof pure and doped ZnO thin films with yttrium doping concentrations 1, 3 and 5 wt%. From the figure, we observed that all the peaks at different 2θ values match well with the JCPDS card no 36-1451 which confirms the wurtzite (hexagonal) structure of the ZnO. The diffraction peaks are at the angles 31.82°, 34.53°, 36.25°, 47.66°, 57.12°, 63.20° and 68.32° correspond to the Miller indices (100), (002), (101), (102), (110), (103) and (112), respectively. No secondary peaks related to yttrium as well as no shift in XRD peaks were observed which may be due to the low doping concentration of yttrium. From Fig.1, it is clearly observed that the preferential growth of ZnO:Y is along (002) plane. The intensity of this preferential orientation decreases as the yttrium doping level increases which may be due to the deterioration of crystallinity [31]. This reduction in intensity may be due to the possible movement of zinc atoms into interstitial sites from the regular zinc locations caused by the substitution of yttrium ions [32]. Scherrer's formula was applied for calculating the crystallite size (D),

$$D = \frac{0.94\,\lambda}{\beta\,cos\theta} \qquad (1)$$

Dislocation density and lattice parameters can be calculated using the formula,

$$\frac{1}{d^2} = \frac{4}{3}\frac{(h^2+k^2+hk)}{a^2} + \frac{l^2}{c^2} \qquad (2)$$

$$\delta = \frac{1}{D^2} \qquad (3)$$

The calculated values of crystallite size are presented in Table 1. We noticed that the crystallite size gradually decreases with the increase of yttrium doping level. This may be due to the incorporation of Y^{3+}(0.89 Å) into Zn^{2+} (0.74 Å) site which causes deformation in the lattice system. This deformation in turn can lead to the restriction of growth of crystallite boundaries

called Zener pinning effect [33]. Rietveld refinement analysis was performed using Bruker Topas version 6 to study the lattice parameters. From Table 1, it can be seen that there is a slight change in the lattice parameter values after doping which may be attributed to the difference in the ionic radii of zinc and yttrium ions. The observed increase in the value of dislocation density with the increase in doping concentration of yttrium shows the formation of defects on the surface of the film [34]. Reduction in the size of the crystallites and the increase in the defects will help for adsorbing more ammonia molecules [35].

3.2 Surface morphological study

Figure 2 shows the AFM images of the pure and yttrium (1, 3 and 5 wt%) doped ZnO films. From the figure, we can observe clear edges of the grains which are generally highly reactive when exposed to target gases. This is one of the main advantages in gas sensing applications [36]. The undoped ZnO thin film exhibits relatively low surface roughness, whereas, considerably higher roughness is observed when yttrium is incorporated into ZnO lattice. The roughness value for pure ZnO increases from 26 to 46 nm due to the influence of yttrium doping. This increase in roughness results in more active centres for gas adsorption favouring better sensing as explained by Wenzel's effect [37, 38]. EDX was used to identify the presence of elements in the prepared films. Figure 3a and b shows the EDX spectra which confirms the existence of zinc, oxygen and yttrium in the samples.

3.3 Photoluminescence study

In order to analyse the surface defects, photoluminescence (PL) study was used. Fig. 4 shows the PL spectra and its Lorentz fitting of pure and yttrium doped ZnO films. The emission band observed at 384 nm is related to the transition between the CB and VB [39]. This peak is found to shift to lower wavelength side due to the influence of yttrium doping. The blue-green emission peaks observed at 435 nm (2.84 eV) and 488 nm (2.53 eV) correspond to Zn_i (zinc

interstitials) and singly ionized V_o (oxygen vacancies) as reported by Kumar *et al*. [40] and Radhidevi *et al*. [34]. Thus, the PL study confirms that the electron donor defect concentration increases when yttrium doping concentration is increased, which is favourable for gas sensing as it can be able to attract more number of gas molecules. In our case, the peaks shifted slightly towards the higher wavelength may be attributed to the bond length of Y-O (2.3 Å) is relatively higher than Zn-O (1.89 Å). Therefore, the origin of the emission defects could be varied with respect to metal doping.

3.4 Optical study

Figure 5 shows the extrapolation of the leading edges of the plot to the x-axis giving the energy band gap as per the Tauc's relation,

$$(\alpha h\nu)^2 = A(h\nu - E_g) \quad (4)$$

From the figure, we can observe a slight increase in the energy gap as the yttrium doping concentration increases. This increase in the band gap may be due to the uplift in electron number caused by the Y^{3+} (trivalent) ions incorporation into the ZnO lattice. When, we dope yttrium with ZnO, the Fermi level moves towards the conduction band of ZnO resulting in band gap widening as explained by Moss-Burstein effect [41].

3.5 Sensing characteristics

3.5.1 Selectivity

The sensing response of the prepared sample (ZnO:Y-5wt%) tested towards six reducing vapours under room temperature is shown in Fig. 6. The selectivity study was carried out by keeping the concentration at 100 ppm and the response was calculated using the formula,

$$S = \frac{R_a}{R_g} \quad (5)$$

The response valuesof the films are 4, 7, 10, 16, 22 and 99 for toluene, acetone, isopropanal, ethanol, methanol and ammonia. From the results, we observed that the film shows poor response to toluene, acetone, isopropanol, ethanol, methanol compared to ammonia. The reason for the best response to ammonia may be the electron donating ability of ammonia compared to other tested vapours due to the presence of lone pair of electrons [42].

3.5.2 Sensing characteristics

Figure 7 shows the response and recovery curves of pure and yttrium doped ZnO films exposed to NH_3 vapours (100 ppm) at 32°C. When yttrium doped ZnO thin films were exposed to NH_3 vapour, a rapid change in resistance was observed indicating the response at room temperature. The response values of the films are 22, 39, 52 and 99 for undoped and yttrium (1, 3 and 5 wt%) doped ZnO films, respectively. The corresponding response and recovery times are 52s/11s, 39s/9s, 30s/11s and 29s/7s. Response and recovery times are the time to reach 90% decrease from the base line upon exposure of target gas and the time taken to return back to the base line, respectively.The results show that 5 wt% yttrium doped ZnO film exhibits quick response and recovery times compared to other films. To study further, transient resistance response curves for 5 wt% yttrium doped ZnO films towards different concentrations of NH_3 vapours (from 100-200 ppm) were recorded (Fig.8). From the figure, we found the same fashion of reduction in resistance during the application of NH_3 and increase in resistance as the consequence of removal of NH_3 vapour for all the five cases. This decreasing and increasing nature of the resistance of n-type material shows the stability of the sensor.

Results of recent research works on NH_3 sensing at room temperature are presented in Table 2. Pandeeswari *et al*. reported that β-Ga_2O_3 film exhibits excellent sensing towards NH_3 and fast response/recovery times of 40 s/ 18 s. This rapid response may be due to the catalytic action of β-Ga_2O_3 [42]. .Niu *et al*. reported that P_2O_5 catalyzed covalent triazine frameworks

exhibit short response/recovery times of 54 s/200 s. It may be attributed to the transfer of electrons between triazine ring and NH_3 molecules [43]. According to Yan *et al.,* Ag_3PO_4 nanoparticles exhibit superior sensing activity towards NH_3. The reason may be the lone pair of NH_3 molecules that coordinate with the atoms of Ag_3PO_4, resulting in a large adsorption of energy and electron transferring [44]. Kathwate *et al.* reported that Al doped ZnO thin films exhibit fast response/recovery times of 29 s/ 19 s that might be attributed to the structural and morphological changes occurred due to Al doping [45]. In the present work, yttrium doped ZnO thin films exhibit short response/recovery times of 29 s/ 7 s towards NH_3 vapours.

3.5.3 Repeatability and stability

Repeatability, one of the important factors in sensing, was tested for 5 wt% yttrium doped ZnO film sensor for five cycles of NH_3 (100 ppm). We found that the response of the sensor remains the same for all the five cycles as shown in Fig. (9a) indicating that the prepared ZnO:Y film (with 5wt% doping) is a good sensing material for sensing NH_3 vapours.

The stability of the sensor is another essential parameter in vapour sensing. To determine the stability, 5 wt% yttrium doped ZnO sensor was tested after 50 days of its preparation with NH_3 vapours (100 ppm) at 32^{o}C. Figure 9b shows that the response of the sensor is nearly the same even after 50 days.

3.5.5 Sensing mechanism

Gas sensing is a surface controlled reactionin which change in resistance of the sensor might be attributed to the adsorption and desorption of target vapours (Fig.10). The adsorbed oxygen molecules can form three types of ions (O_2^--below 100^{o}C(equation 6), O^- -between 100^{o}C to 300^{o}C and O^{2-} -above 300^{o}C). Previous reports showed the formation of O_2^-ions on the film surface at room temperature [40]. In the present study, we believe that these oxygen ions

form a depletion layer over the surface of ZnO:Y films and thus resulting in a high electrical resistance.

$$O_2 + e^- = O_{2\,(ads)}^- \quad (6)$$

Upon exposure to NH_3 vapours, desorption takes place and concomitantly electrons already trapped are released back to the film which results in reduction in resistance as per the equation (7). As ZnO is an n-type material having a wide band gap, large number of oxygen ions are adsorbed on the ZnO:Y film surface. Oxygen vacancies and zinc interstitials are donor defects favouring the adsorption of oxygen ions and consequently increase the interaction of NH_3 molecules with the sensing surface. The higher the donor defects the higher is the adsorption of oxygen molecules which leads to an increase in the sensing response as evidenced from the PL results.

$$4NH_3 + O_{2\,(ads)}^- = 2N_2 + 6H_2O + 3e^- \quad (7)$$

4. Conclusion

Yttrium doped ZnO films prepared using cost-effective spray pyrolysis technique exhibit good ammonia vapour sensing. The ZnO sensor with 5 wt% yttrium doping shows superior sensing response (99) and quick response/recovery times of 29 s/ 7 s for 100 ppm of ammonia at 32^{o}C. ZnO:Y (5 wt%) film has more oxygen vacancies and zinc interstitials, which can adsorb more ammonia molecules during sensing. The enhanced sensing response may also be due to the excessive electrons donated by the trivalent (yttrium) ion into the divalent (zinc) lattice. The resultant band gap widening is evidenced by the Moss-Burstein effect. Increase in roughness plays a crucial role in sensing. From the above results, we have concluded that yttrium doped ZnO thin films can be considered as promising candidates for NH_3 sensing.

Acknowledgement

The authors from KSU extend their appreciation for funding part of the work to the Researchers Supporting Project number (RSP-2020/61), King Saud University, Riyadh, Saudi Arabia.

Conflict of interests

The authors declare that they have no conflict of interest.

References

[1] E. Hemalatha, N. Gopalakrishnan, Synthesis and characterization of pure and Cd doped ZrO_2 nanostructures for ammonia sensing application, *Mater. Today.,* https://doi.org/10.1016/j.matpr.2020.06.197

[2] Roto Rotoa, Aditya Rianjanu, Innas Amaliya Fatyadi, Ahmad Kusumaatmaja, Kuwat Triyana, Enhanced sensitivity and selectivity of ammonia sensing by QCM modified with boric acid-doped PVAc nanofiber, *Sens. Actuator A Phys*., **304** (2020) 111902

[3] Susmita Kundu, Amit Kumar, Low concentration ammonia sensing performance of Pd incorporated indium tin oxide, *J Alloy Compd.*,**750** (2019) 245-255

[4] Shobha N. Birajdar, Neha Y. Hebalkar, Satish K. Pardeshi, Sulabha K. Kulkarni, Parag V. Adhyapak, Ruthenium-decorated vanadium pentoxide for room temperature ammonia sensing, *RSC Adv.*, **9** (2019) 28735

[5] S. Maheswari, M. Karunakaran, K. Kasirajan, Nebuliser spray pyrolysis coated undoped and Tb-doped SnO_2 thin films: Ammonia vapour sensor application, *Sustainable Humanosphere*, ISSN: **1880 – 6503** (2020) Volume: 16 Issue: 1

[6] Z.P. Tshabalala, K. Shingange, F.R. Cummings, O.M. Ntwaeaborwa, G.H. Mhlongo, D.E. Motaung, Ultra-Sensitive and Selective NH_3 Room Temperature Gas Sensing Induced by Manganese-doped Titanium Dioxide Nanoparticles, *J. Colloid Interface Sci*., **504** (2017) 371-386

[7] Xiaolan Deng, Lilan Zhang, Jing Guo, Qinjun Chen, Jianmin Ma, ZnO enhanced NiO-based gas sensors towards ethanol, *Mater. Res. Bull.*, **90** (2017) 170-174

[8] Xuesong Wang, Jinbao Zhang, Lianyuan Wang, Shouchun Li, Li Liu, Chang Su, Lili Liu, High Response Gas Sensors for Formaldehyde Based on Er-Doped In_2O_3 Nanotubes, *J Mater Sci Technol.*, **31** (2015) 1175-1180

[9] R.P. Patil, Chaitanya Hiragond, G.H. Jain, Pawan K. Khanna, V.B. Gaikwad, Priyesh V. More, La doped $BaTiO_3$ nanostructures for room temperature sensing of NO_2/NH_3: Focus on La concentration and sensing mechanism, *Vacuum.*, **166** (2019) 37–44

[10] R. Sankar Ganesh, E. Durgadevi, M. Navaneethan, V.L. Patil, S. Ponnusamy, C. Muthamizhchelvan, S. Kawasaki, P.S. Patil, Y. Hayakawa, Controlled synthesis of Ni-doped ZnO hexagonal microdiscs and their gas sensing properties at low temperature, *Chem. Phys. Lett*., **689**(2017) 92-99

[11] A. Manivasaham, K. Ravichandran, K. Subha: Light intensity effects on the sensitivity of ZnO:Cr gas sensor, *Surf. Eng.*, **33** (2017) Issue 11

[12] V.L. Patil, S.A. Vanalakar, N.L. Tarwal, A.P. Patil, T.D. Dongale, J.H. Kim, P.S. Patil, Construction of Cu doped ZnO nanorods by chemical method for Low temperature detection of NO_2 gas, *Sens. Actuator A Phys*., **299** (2019) 111611

[13] A. Jansi Santhosam, K. Ravichandran, Mohd. Shkir, M. Sridharan, Effect of La incorporation on the NH_3 sensing behaviour of ZnO thin films prepared using low-cost nebulizer spray technique, *J. Mater. Sci.: Mater. Electron*., **31** (2020) 13240-13248

[14] M. Rajendra Prasad, M. Haris, M. Sridharan, NH_3 sensing properties of surface modified Ce-doped nanostructured ZnO thin films prepared by spray pyrolysis method, *Sens. Actuator A Phys.*, **269** (2018) 435–443
[15] Singh G, Virpal, Singh RC, Highly sensitive gas sensor based on Er-doped SnO_2 nanostructures and its temperature dependent selectivity towards hydrogen and ethanol, *Sensor Actuat B-Chem*., **282** (2019) 373-383
[16] Anita Hastir, Nipin Kohli, Ravi Chand Singh, Temperature dependent selective and sensitive terbium doped ZnO nanostructures, *Sensor Actuat B-Chem.*, **231** (2016) 110-119
[17] V. Anand, A. Sakthivelu, K. Deva Arun Kumar, S. Valanarasu, V. Ganesh, Mohd. Shkir, A. Kathalingam, S. AlFaify, Novel rare earth Gd and Al co-doped ZnO thin films prepared by nebulizer spray method for optoelectronic applications, *Super lattice Microst*., **123** (2018) 311-322
[18]Narinder Kaur, Sanjeev K. Sharma, Deuk Young Kim, Narinder Singh, *Physica B Condens. Matter.,* **500** (2016) 179-185
[19] K. Deva Arun Kumar, S. Valanarasu, Joice Sophia Ponraj, Brian Jeevan Fernandes, M. Shkir, S. AlFaify, Prashantha Murahari, K. Ramesh, Effect of Er doping on the ammonia sensing properties of ZnO thin films prepared by a nebulizer spray technique, *J. Phys. Chem. Solids.*, **144** (2020) 109513
[20] Haiyu Qin, Jing Xie, Hui Xu, Yizhao Li, Yali Cao, Green solid-state chemical synthesis and excellent xylene detecting behaviors of Y-doped-MoO_3 nanoarrays, *Mater Res Bull.*, **93** (2017) 256-263
[21] X.B. Li, Q.Q. Zhang, S.Y. Ma, G.X. Wan, F.M. Li, X.L. Xu, Microstructure optimization and gas sensing improvement of ZnO spherical structure through yttrium doping, *Sensor Actuat B-Chem.*, **195** (2014) 526–533
[22] N. Nithya, G. Bhoopathi, G. Magesh, O.N. Balasundaram, Synthesis and characterization of yttrium doped titania nanoparticles for gas sensing activity, *Mater. Sci. Semicond. Process.*, **99** (2019) 14–22
[23] Julakanti Shruthi, Nagabandi Jayababu, P. Ghosal, M.V. Ramana Reddy, Ultrasensitive sensor based on Y_2O_3-In_2O_3 nanocomposites for the detection of methanol at room temperature, *Ceram. Int*., **45** (2019) 21497–21504
[24] Veena Mounasamy, Ganesh Kumar Mani, Dhivya Ponnusamy, Kazuyoshi Tsuchiya, Arun K. Prasad, Sridharan Madanagurusamy, Sub-ppm level detection of tri-methylamine using V_2O_3-Cu_2O mixed oxide thin films, *Ceram.Int.*, **45** (2019) 19528–19533
[25] R.Sankar Ganesh, E.Durgadevi, M.Navaneethan, V.L.Patil, S.Ponnusamy, C.Muthamizhchelvan, S.Kawasaki, P.S.Patil, Y.Hayakawa, Tuning the selectivity of NH_3 gas sensing response using Cu-doped ZnO nanostructures, *Sens. Actuator A Phys.*, **269** (2018) 331-341
[26]Poloju, M, Jayababu. N, Ramana Reddy M. V., Improved gas sensing performance of Al doped ZnO/CuO nanocomposite based ammonia gas sensor, *MSEB.*, **227** (2017) 61–67
[27]Salvatore Gianluca Leonardi , Wojtek Wlodarski , Yongxiang Li, Nicola Donato, Anna Bonavita , Giovanni Neri, Ammonia sensing properties of two-dimensional tin disulphide/tin oxides (SnS_2/SnO_{2-x}) mixed phases, *J Alloy Compd*., **781** (2019) 440-449
[28] K.Radhi Devi, G. Selvan, M. Karunakaran, K. Kasirajan, Mohd. Shkir, S. Alfaify,A SILAR fabrication of nanostructured ZnO thin films and their characterizations for gas sensing applications: An effect of Ag concentration, *Super lattice Microst*., **143** (2020) 106547

[29] V.Gopala Krishnan, P.Elango, Influence of Ba doping concentration on the physical properties and gas sensing performance of ZnO nanocrystalline films: Automated nebulizer spray pyrolysis (ANSP) method, *Optik.*, **141** (2017) 83-89

[30] K. Ravichandran, K. Subha, N. Dineshbabu, A. Manivasaham, Enhancing the electrical parameters of ZnO films deposited using a low-cost chemical spray technique through Ta doping, *J Alloy Compd*., **656** (2016) 332-338
[31] K. Karthika, K. Ravichandran, Tuning the Microstructural and Magnetic Properties of ZnO Nanopowders Through the Simultaneous Doping of Mn and Ni for Biomedical Applications, *J Mater Sci Technol*., **31**(2015) 1111-1117
[32]K. Karthika, K.Ravichandran, Enhancing the magnetic and antibacterial properties of ZnO nanopowders through Mn+Co doping, *Ceram.Int*., **41** (2015) 7944-7951
[33]K. Ravichandran, A. Manivasaham, Enhanced ammonia sensing by Sn doped ZnO films prepared by a low-cost fully automated nebulizer spray technique, *J Mater Sci: Mater Electron.*, **28** (2017) 6335-6344
[34] K. Radhi Devi, G. Selvan , M. Karunakaran , I. Loyola Poul Raj , V. Ganesh, S. AlFaify, Enhanced room temperature ammonia gas sensing properties of strontium doped ZnO thin films by cost-effective SILAR method, *Mater. Sci. Semicond. Process*., **119** (2020) 105117
[35] Rekha Pilliadugula, N. Gopala Krishnan, Effect of pH dependent morphology on room temperature NH_3 sensing performances of β-Ga_2O_3, *Mater. Sci. Semicond. Process*., **112** (2020) 105007
[36] Veena Mounasamy, Ganesh Kumar Mani, Dhivya Ponnusamy, Kazuyoshi Tsuchiya, Arun K. Prasad, Sridharan Madanagurusamy, Network mixed metal oxide (V^{4+} and Ti^{4+}) nanostructures as potential material for the detection of tri-methylamine, *New J. Chem.*, **43** (2019) 11069
[37] Veena Mounasamy, Ganesh Kumar Mani, Dhivya Ponnusamy, Kazuyoshi Tsuchiya, Arun K. Prasad, Sridharan Madanagurusamy, Template-free synthesis of vanadium sesquioxide (V_2O_3) nanosheets and their room-temperature sensing performance, *J. Mater. Chem.A.*, **6** (2018) 6402
[38] Yaoyu Yin, Yanbai Shen, Pengfei Zhou, Rui Lu, Ang Li, Sikai Zhao, Wengang Liu, Dezhou Wei, Kefeng Wei, Fabrication, characterization and n-propanol sensing properties of perovskite-type $ZnSnO_3$ nanospheres based gas sensor, *Appl Surf Sci*., **509** (2020) 145335
[39] K. Ravichandran, K. Shantha Seelan, P. Kavitha, S. Sriram, Influence of Cu+ g-C_3N_4 incorporation on the photocatalytic dye decomposition of ZnO film coated on stainless steel wire meshes, *J Mater Sci: Mater Electron.*, **30** (2019) 19703-19717
[40] A. Jansi Santhosam, K. Ravichandran, Tansir Ahamad, *Sens.Actuator A Phys.,* **316** (2020) 112376
[41] Weiwei Guo, Tianmo Liu, Rong Sun, Yong Chen, Wen Zeng, Zhongchang Wang, Hollow, porous, and yttrium functionalized ZnO nanospheres with enhanced gas-sensing performances, *Sensor Actuat B-Chem*., **178** (2013) 53– 62
[42] R. Pandeeswari, B.G. Jeyaprakash, High sensing response of β-Ga_2O_3 thin film towards ammonia vapours: Influencing factors at room temperature, *Sensor Actuat B-Chem.*, **195** (2014) 206–214
[43] Fang Niu, Zhen-Wu Shao, Li-Ming Tao, Yong Ding, Covalent triazine-based frameworks for NH_3 gas sensing at room temperature, *Sensor Actuat B-Chem.*, **321** (2020) 128513
[44] Fanfan Yan, Guowen Shen, Xi Yang, Tianjiao Qi, Jie Sun, Xinghua Li, Mingtao Zhang, Low operating temperature and highly selective NH_3 chemi-resistive gas sensors based on Ag_3PO_4 semiconductor, *Appl Surf Sci*., **479** (2019) 1141–1147
[45] L.H. Kathwate, G. Umadevi, P.M. Kulal, P. Nagaraju, D.P. Duba, A.K. Nanjundan, V.D. Mote, Ammonia Gas sensing properties of Al doped ZnO thin films, *Sens. Actuator A Phys.*, **313** (2020) 112193
[46] Ali Akbar, Mausumi Das, D. Sarkar, Room temperature ammonia sensing by CdS nanoparticle decorated polyaniline (PANI) nanorods, *Sens. Actuator A Phys.*, **310** (2020) 112071

[47] Wang W, Zhen Y, Zhang J, Li Y, Zhong H, Jia Z, Xiong Y, XueQ,Yan Y, Alharbib NS, Hayat T, SnO_2 nanoparticles-modified 3D-multilayer MoS_2 nanosheets for ammonia gas sensing at room temperature, *Sensor Actuat B-Chem.*, **321**(2020) 128471
[48] Yuli Zhou, Jian Wang, Xinkang Li, Flexible room-temperature gas sensor based on poly (para-phenyleneterephthalamide) fibers substrate coupled with composite NiO@CuO sensing materials for ammonia detection, *Ceram. Int*., **46** (2020) 13827-13834
[49] P.G.Su, L.Y.Yang, NH_3 gas sensor based on Pd/SnO_2/RGO ternary composite operated at room-temperature, *Sens. Actuators B Chem.,* **223** (2016) 202-208

Figure Captions

Fig.1 X-ray diffraction patterns of ZnO and ZnO:Y thin films

Fig.2 AFM images of ZnO:Y thin films with different Y loading levels a) 0 b) 1 c) 3 and d) 5wt%

Fig.3 (a,b) EDX spectra of ZnO and ZnO:Tb (5wt%) thin films

Fig.4 Photoluminescence spectra of ZnO and Y doped ZnO thin films

Fig.5 Tauc's plot of ZnO and ZnO:Y (1, 3 and 5 wt%) thin films to measure the bandgap

Fig.6 Selectivity of ZnO:Y-5wt% thin film towards various test vapours

Fig.7 Response and recovery curves of ZnO:Y (0, 1, 3 and 5 wt%) thin films towards 100 ppm of NH_3 at room temperature

Fig.8 Response and recovery curves of 5 wt% yttrium doped ZnO thin film towards various concentrations of NH_3

Fig.9.a) Repeatability curve of 5 wt% yttrium doped ZnO thin films **b)** Stability curve of ZnO:Y (0, 1, 3 and 5 wt%) thin films over 50 days

Fig.10 Sensing mechanism of ZnO:Y thin film

Table Captions

Table 1 Crystallite size, Lattice parameters and dislocation density of ZnO:Y (0, 1, 3 and 5 wt%) thin films

Table 2 Response/recovery times and sensitivity of various materials towards NH_3 sensing

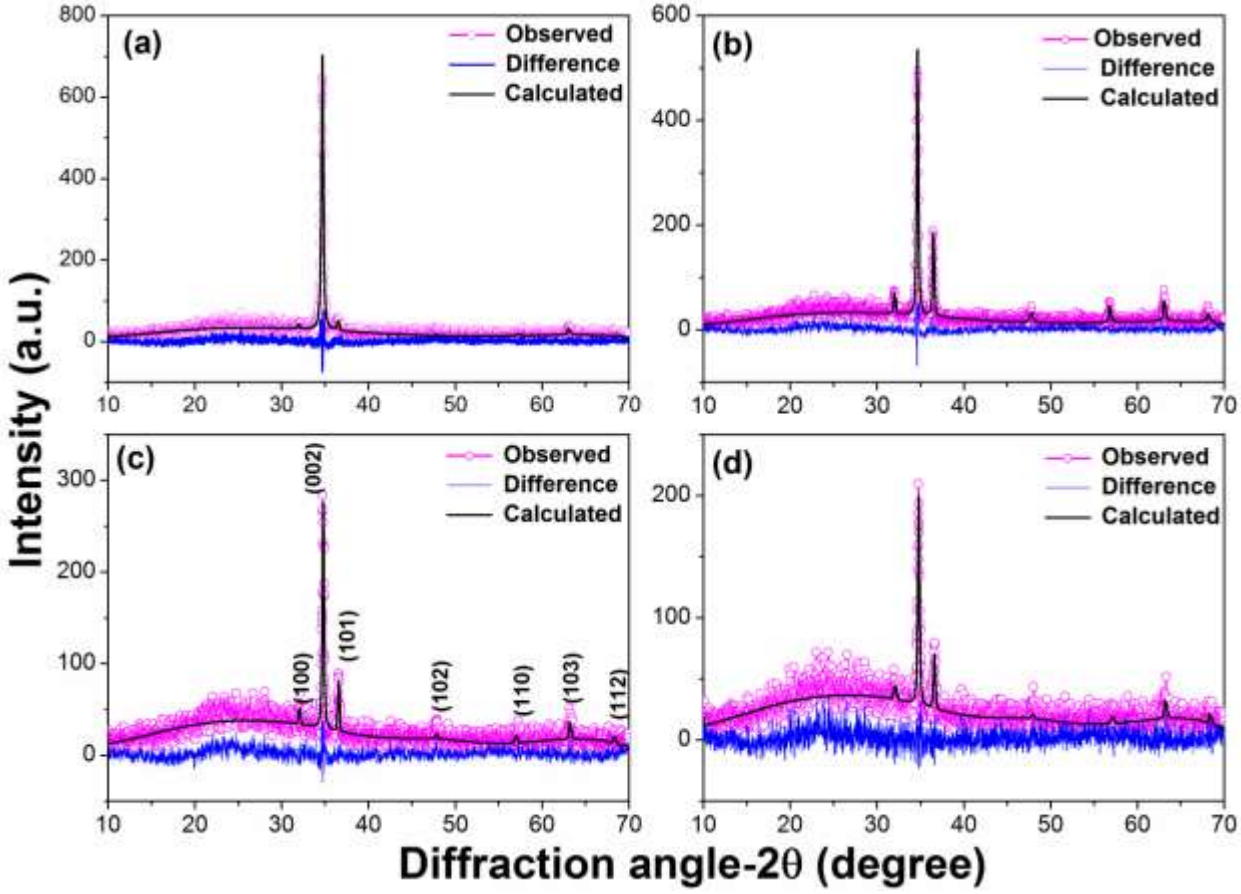
(a)
(b)
(c)
(d)
Observed
Difference
Calculated
(100)
(002)
(101)
(102)
(110)
(103)
(112)
Intensity (a.u.)
Diffraction angle-2θ (degree)

Fig.1

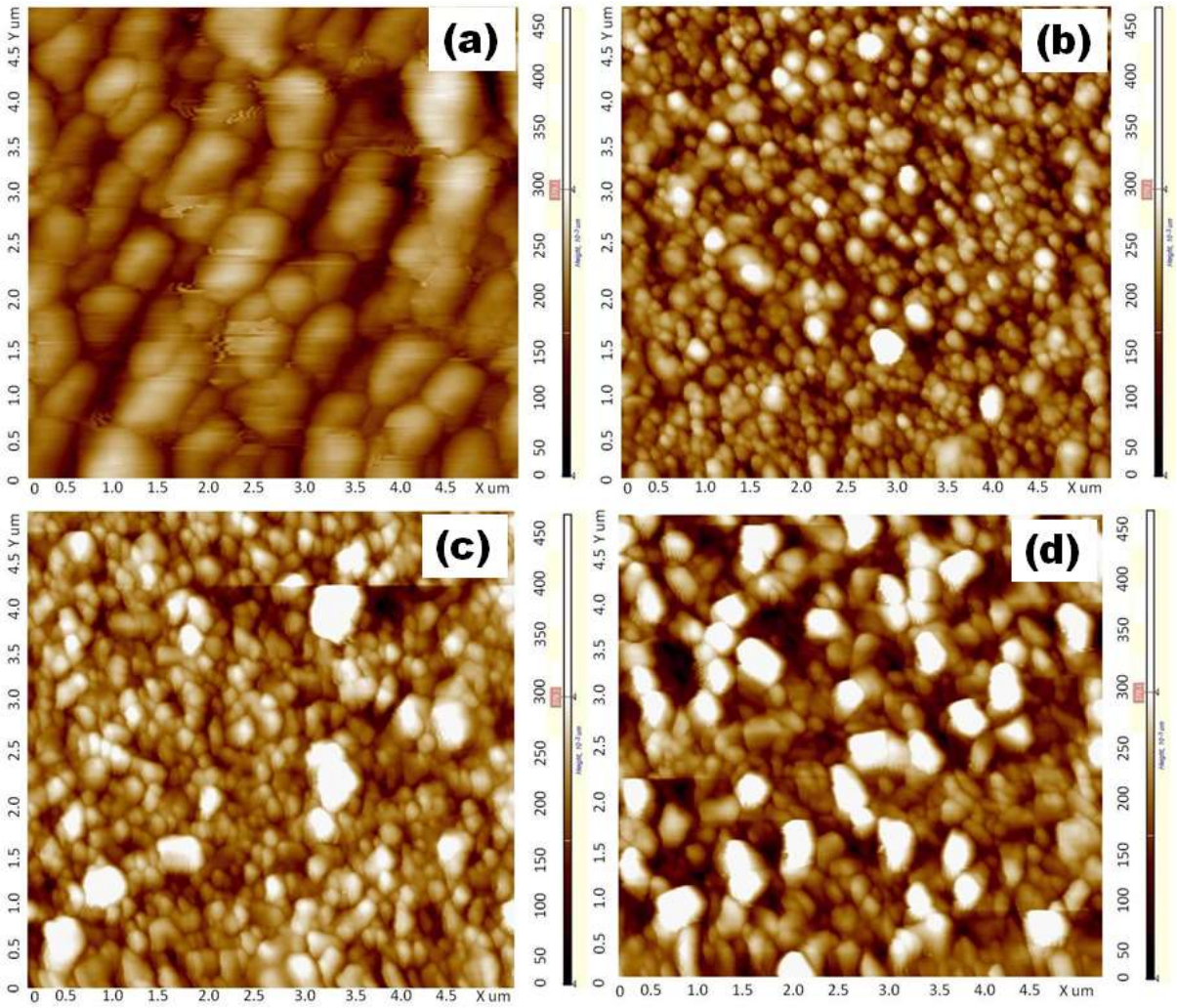
(a)
(b)
(c)
(d)
0 0.5 1.0 1.5 2.0 2.5 3.0 3.5 4.0 4.5 X um
0 0.5 1.0 1.5 2.0 2.5 3.0 3.5 4.0 4.5 Y um
0 50 100 150 200 250 300 350 400 450

Fig.2

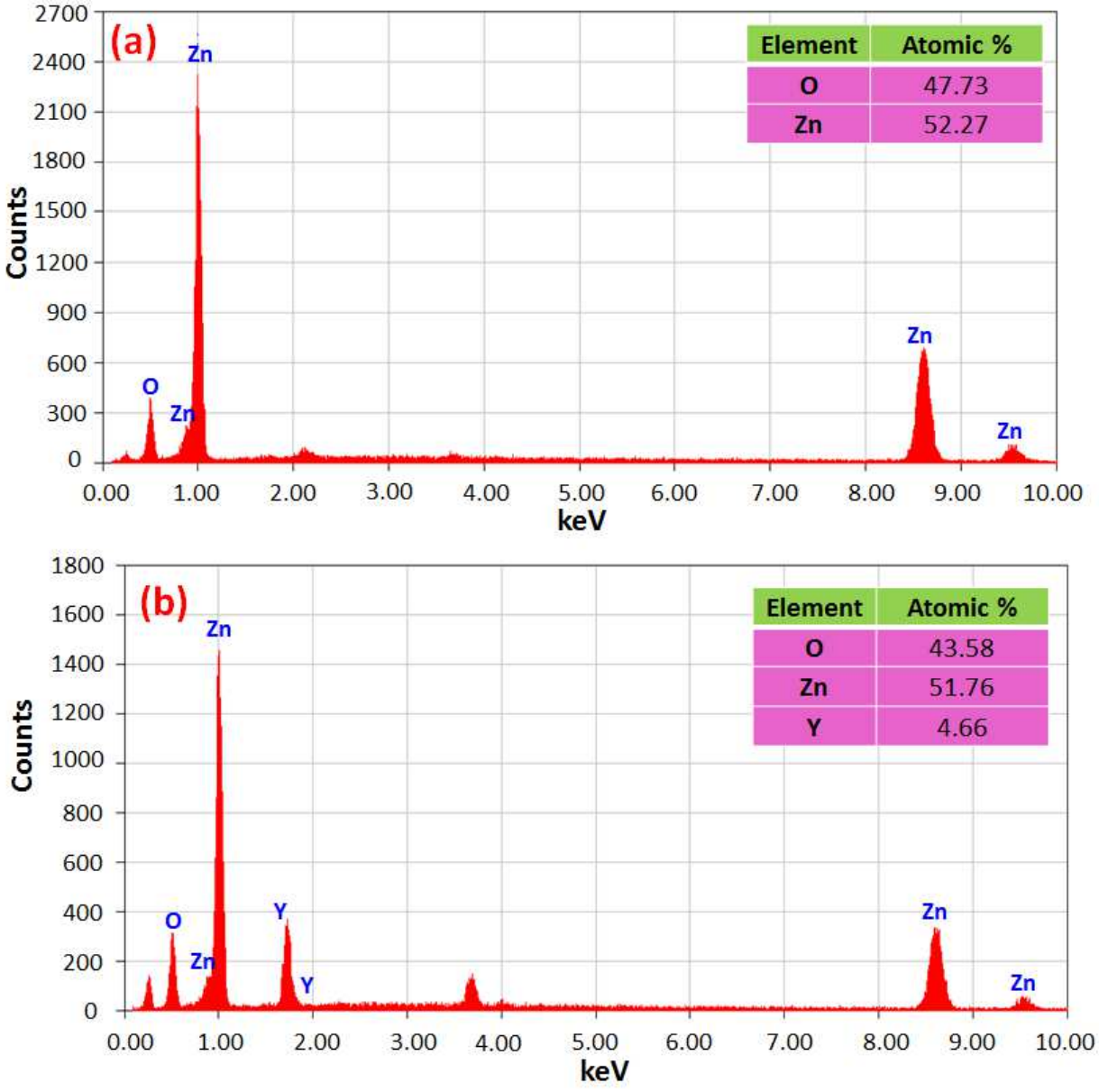
(a)
Element
Atomic %
O
47.73
Zn
52.27
Counts
keV
Zn
O
Zn
Zn
Zn
(b)
Element
Atomic %
O
43.58
Zn
51.76
Y
4.66
Counts
keV
Zn
O
Zn
Y
Y
Zn
Zn

Fig.3

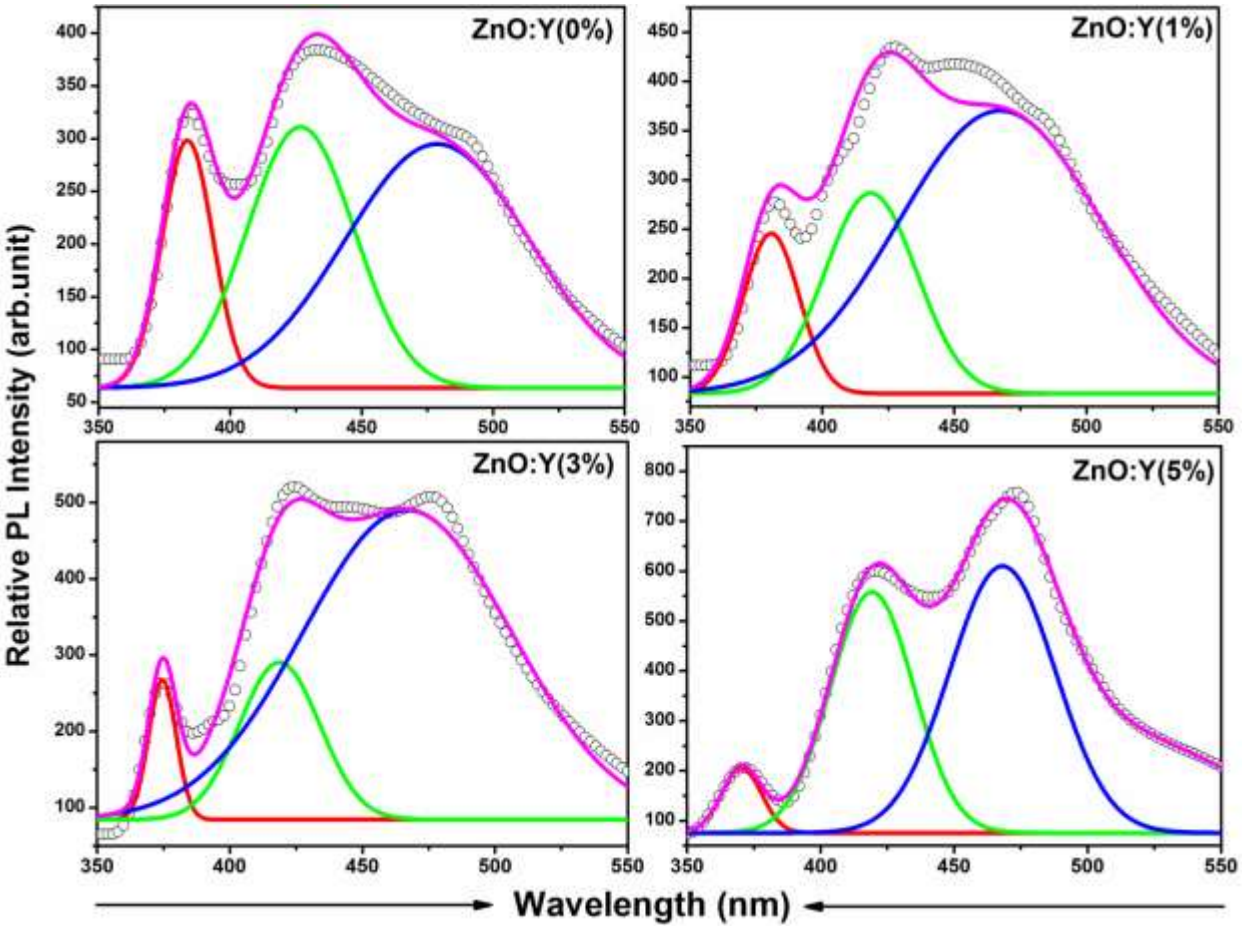
ZnO:Y(0%)
ZnO:Y(1%)
ZnO:Y(3%)
ZnO:Y(5%)
Relative PL Intensity (arb.unit)
Wavelength (nm)

Fig.4

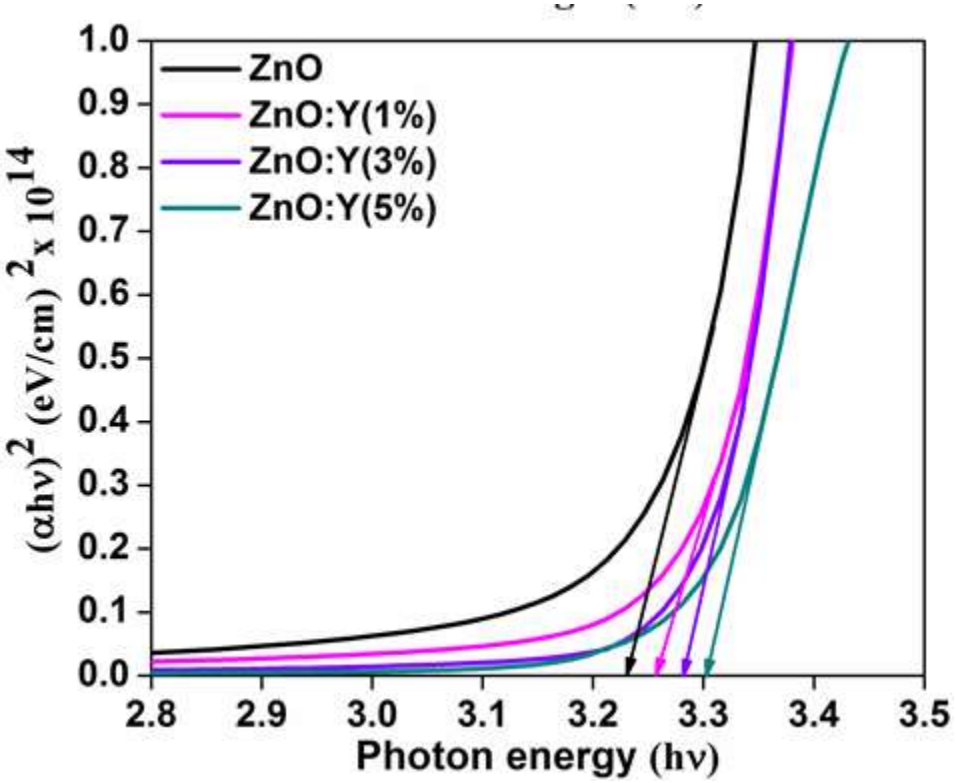
ZnO
ZnO:Y(1%)
ZnO:Y(3%)
ZnO:Y(5%)
(αhν)2 (eV/cm) 2x 1014
Photon energy (hν)
1.0
0.9
0.8
0.7
0.6
0.5
0.4
0.3
0.2
0.1
0.0
2.8
2.9
3.0
3.1
3.2
3.3
3.4
3.5

Fig.5

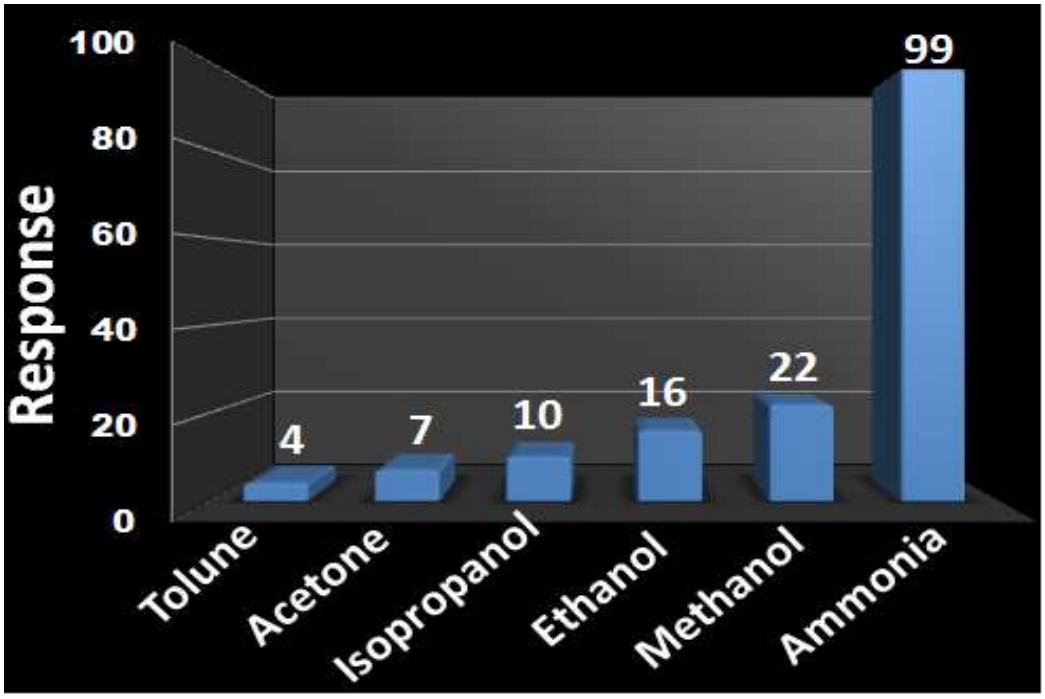
Response
100
80
60
40
20
0
4
7
10
16
22
99
Tolune
Acetone
Isopropanol
Ethanol
Methanol
Ammonia

Fig.6

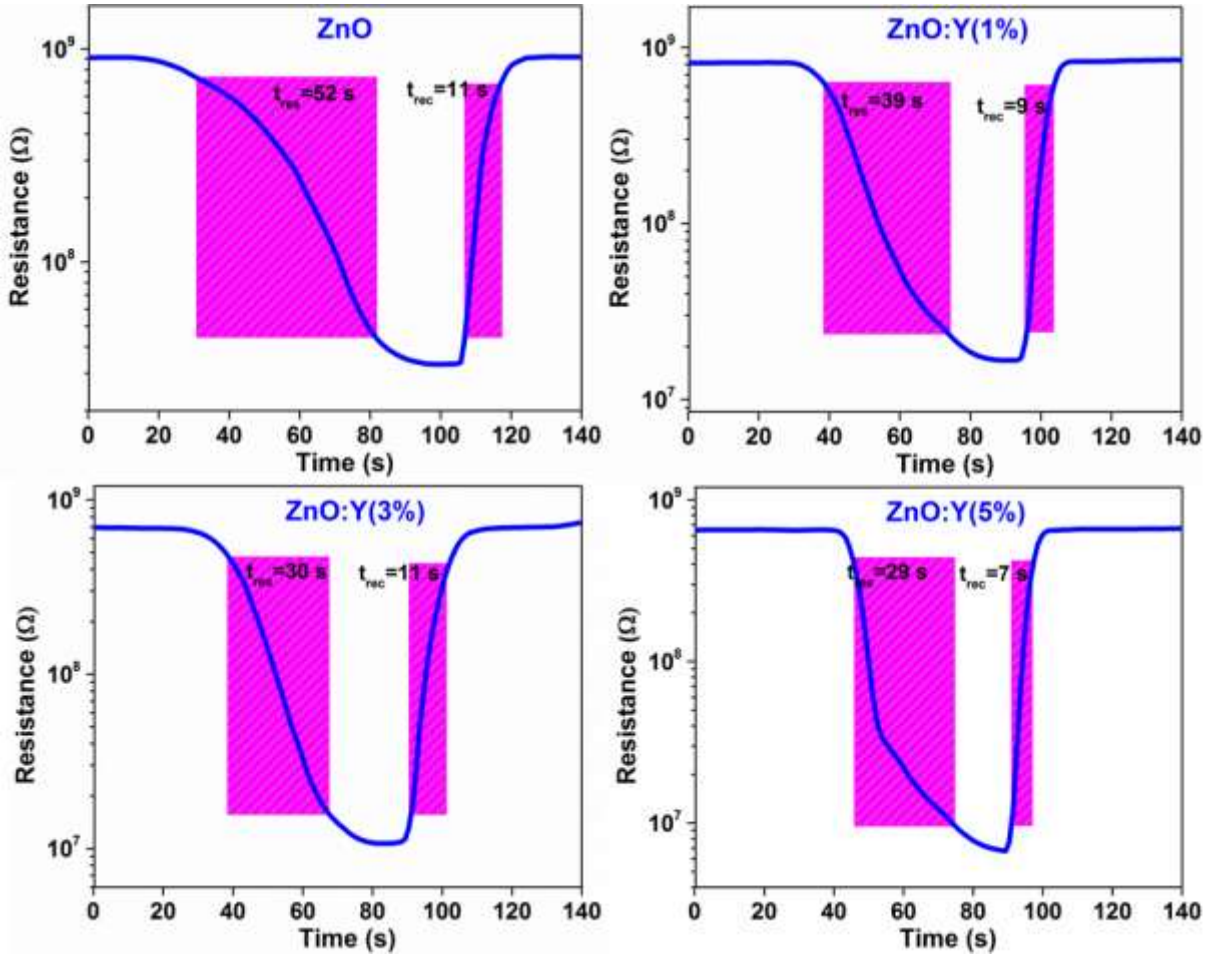
ZnO
t_{res}=52 s
t_{rec}=11 s
ZnO:Y(1%)
t_{res}=39 s
t_{rec}=9 s
ZnO:Y(3%)
t_{res}=30 s
t_{rec}=11 s
ZnO:Y(5%)
t_{res}=29 s
t_{rec}=7 s
Resistance (Ω)
Time (s)

Fig.7

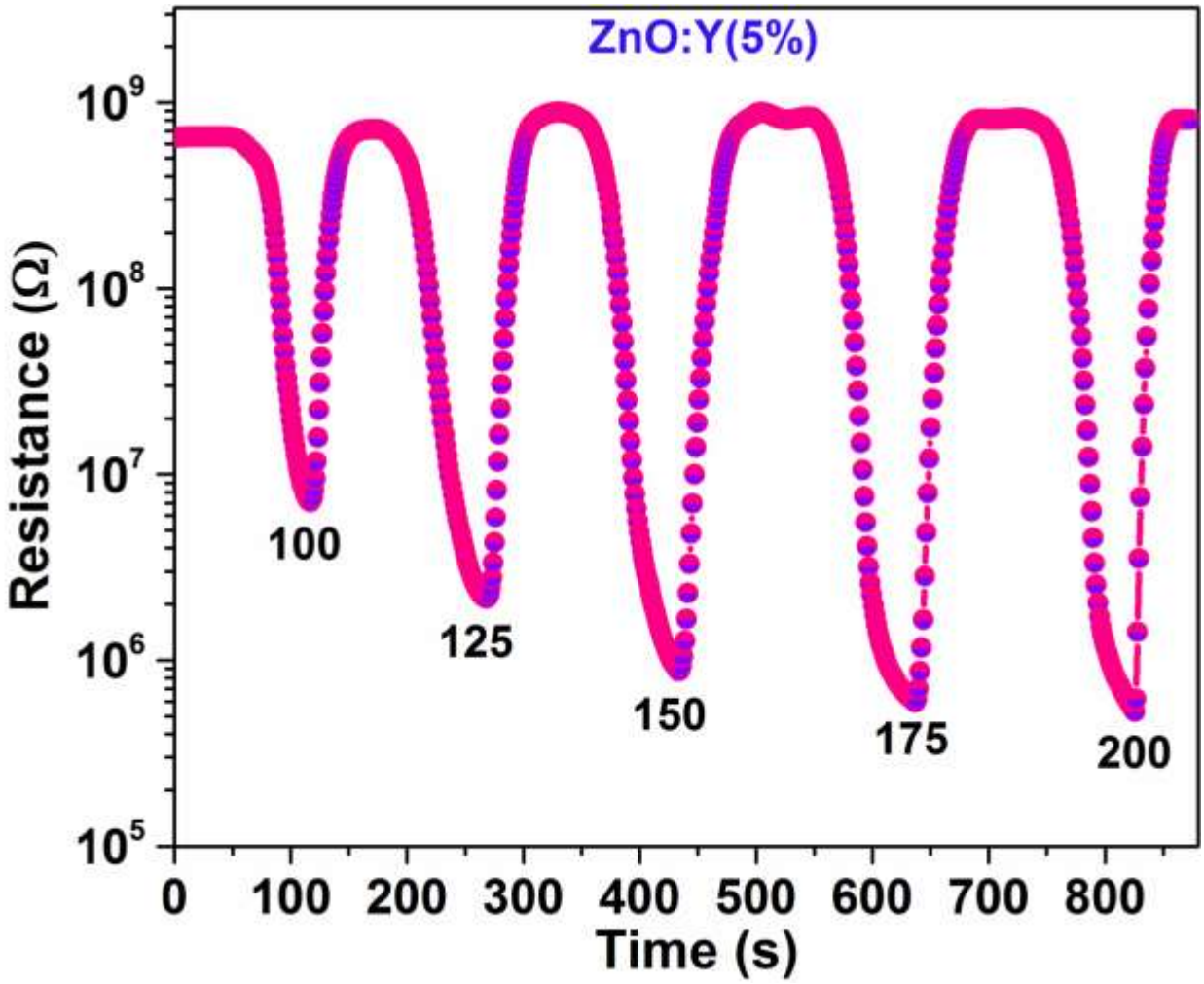
ZnO:Y(5%)
Resistance (Ω)
10^9
10^8
10^7
10^6
10^5
100
125
150
175
200
0
100
200
300
400
500
600
700
800
Time (s)

Fig.8

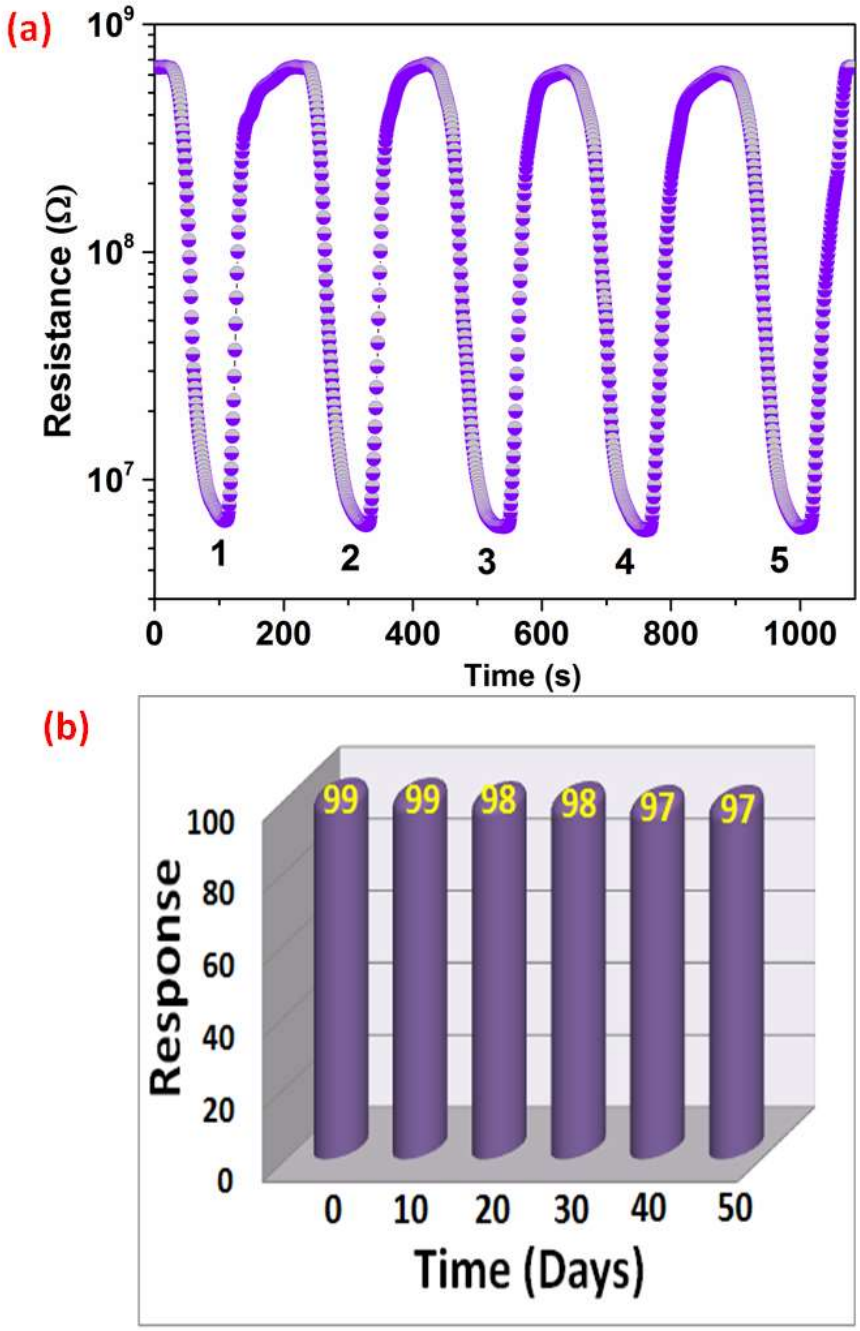
(a)
Resistance (Ω)
10^9
10^8
10^7
1
2
3
4
5
0
200
400
600
800
1000
Time (s)
(b)
Response
100
80
60
40
20
0
99
99
98
98
97
97
0
10
20
30
40
50
Time (Days)

Fig.9 a and b

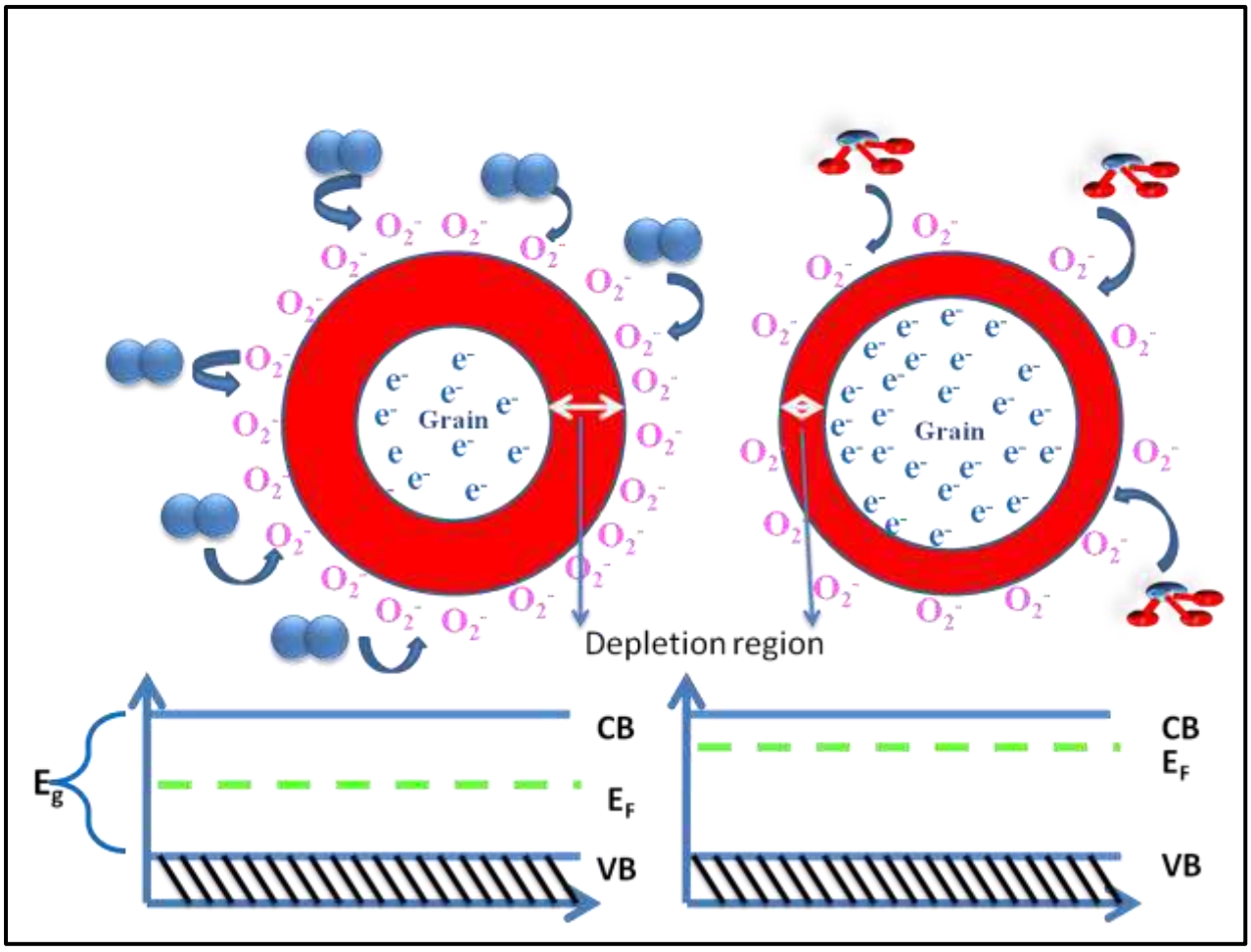
Grain
Grain
Depletion region
CB
E_F
VB
E_g
CB
E_F
VB

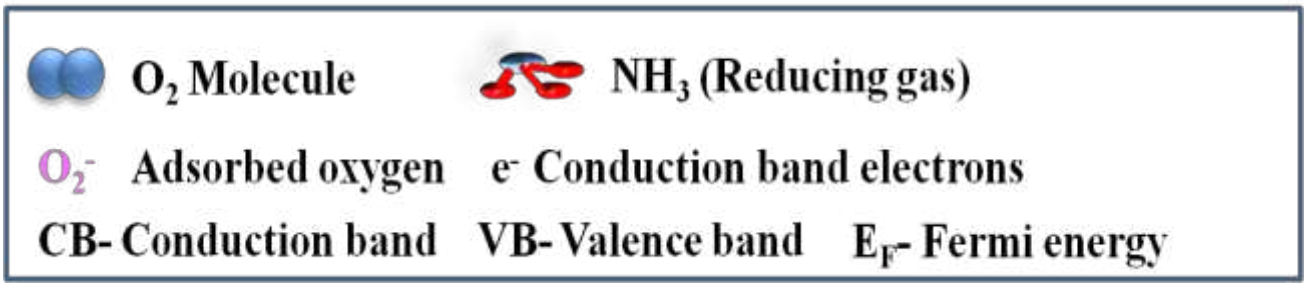
O_2 Molecule
NH_3 (Reducing gas)
O_2^- Adsorbed oxygen
e^- Conduction band electrons
CB- Conduction band
VB- Valence band
E_F- Fermi energy

Fig.10

Table 1

Samples	Lattice parameters		Crystallite size D (nm)	Dislocation density δ(x10^{15} lines/m^2)	Film thickness (nm)
	a (Å)	c (Å)			
ZnO	3.222 (5)	5.231 (9)	32	0.976	350
ZnO:Y (1%)	3.185 (2)	5.173 (8)	30	1.111	340
ZnO:Y(3%)	3.186 (13)	5.155 (5)	29	1.189	330
ZnO:Y (5%)	3.179 (2)	5.136 (9)	26	1.479	320

Table 2

Material	Method	Sensing Temperature	Concentration (ppm)	Response (S)	Response time(s)	Recovery time(s)	Ref.
Sr doped ZnO	SILAR	RT	100	-	22	6	[34]
β-Ga_2O_3	Spray pyrolysis	RT	0.5-50	19-33,250	40	18	[42]
P_2O_5 catalyzed triazine frameworks	-	RT	50	3.3%	54	200	[43]
CdS decorated PANI	Chemical co-dispersion	RT	20-100	250	58	104	[46]
SnO_2/MoS_2	Hydrothermal	RT	50	2080.36	23	1.6	[47]
NiO/CuO	Electroless deposition	RT	20	-	72.5	35	[48]
Pd/SnO_2/RGO	One pot route	RT	100	19.6	420	3000	[49]
Yttrium doped ZnO	Nebulizer spray Pyrolysis	RT	100	99	29	7	Present work

Figures

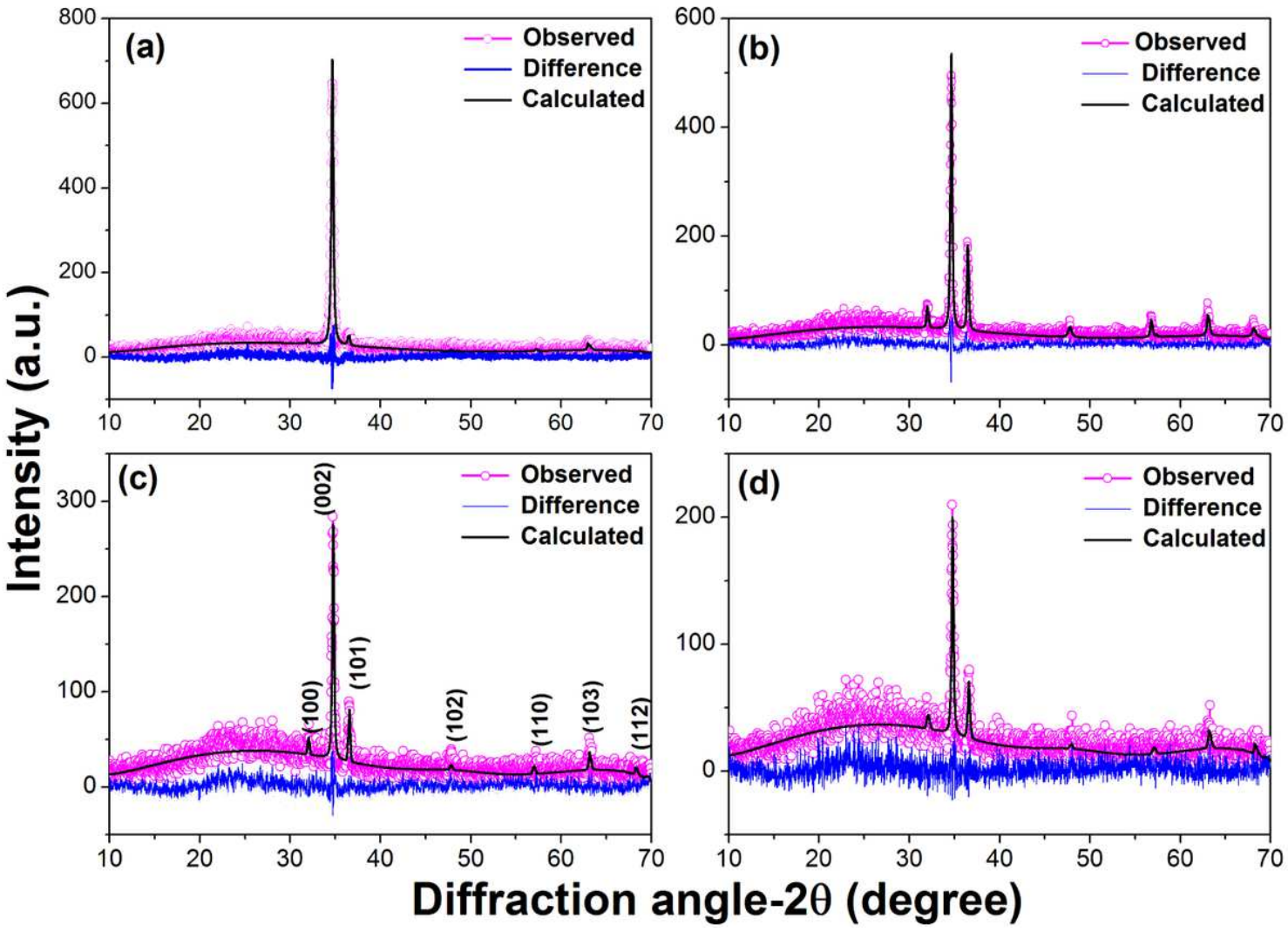

Figure 1

X-ray diffraction patterns of ZnO and ZnO:Y thin films

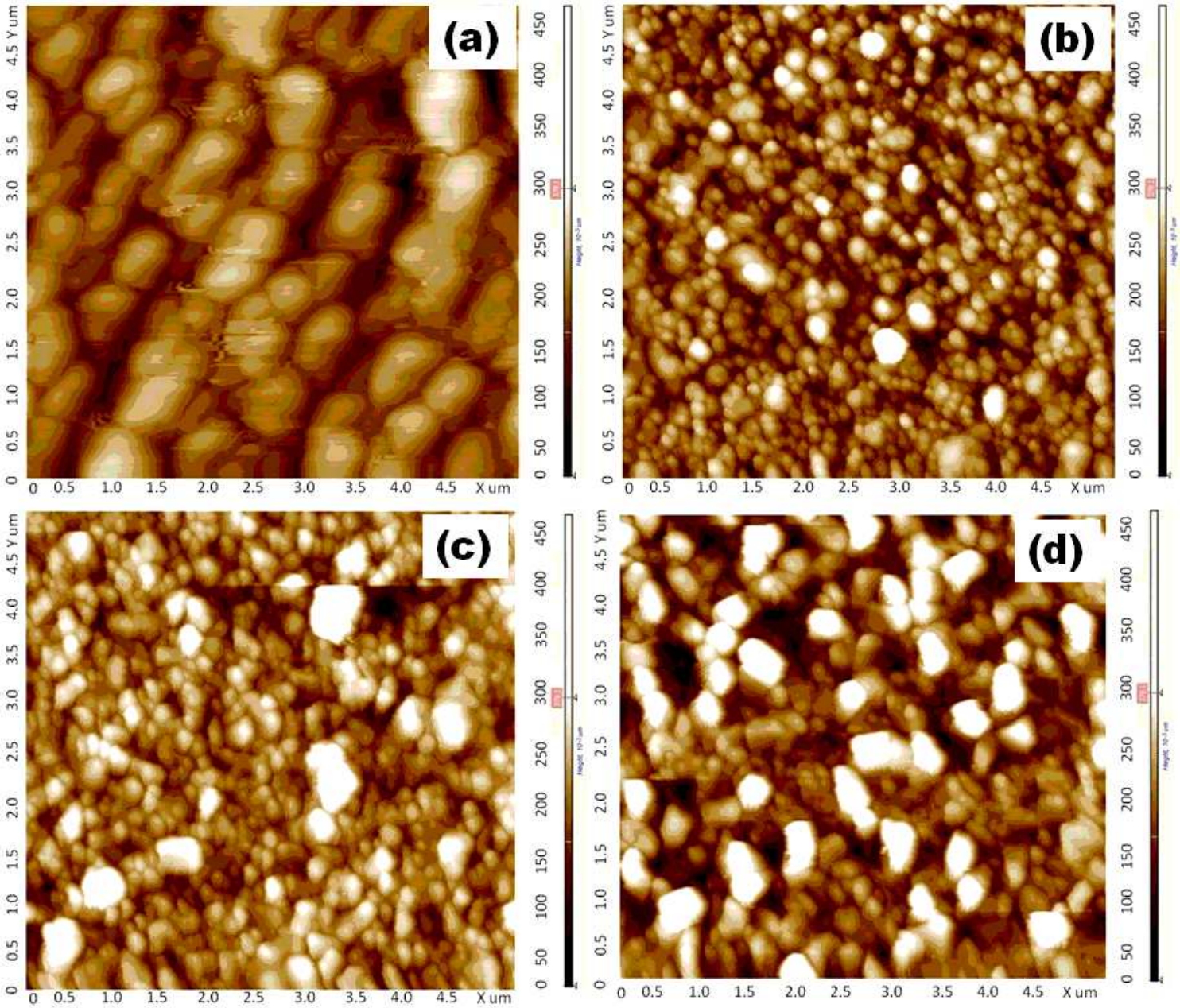

Figure 2

AFM images of ZnO:Y thin films with different Y loading levels a) 0 b) 1 c) 3 and d) 5wt%

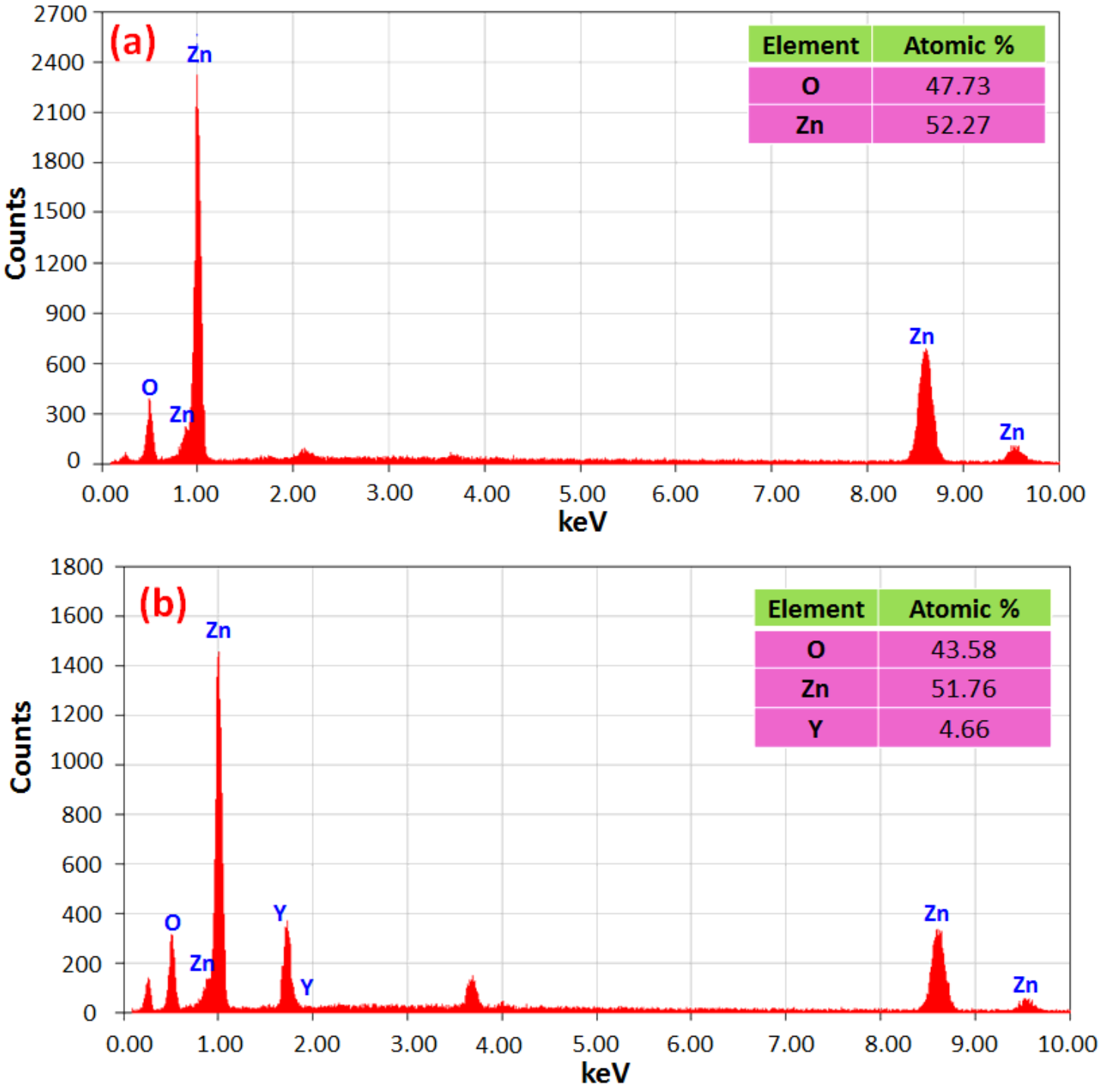

Figure 3

(a,b) EDX spectra of ZnO and ZnO:Tb (5wt%) thin films

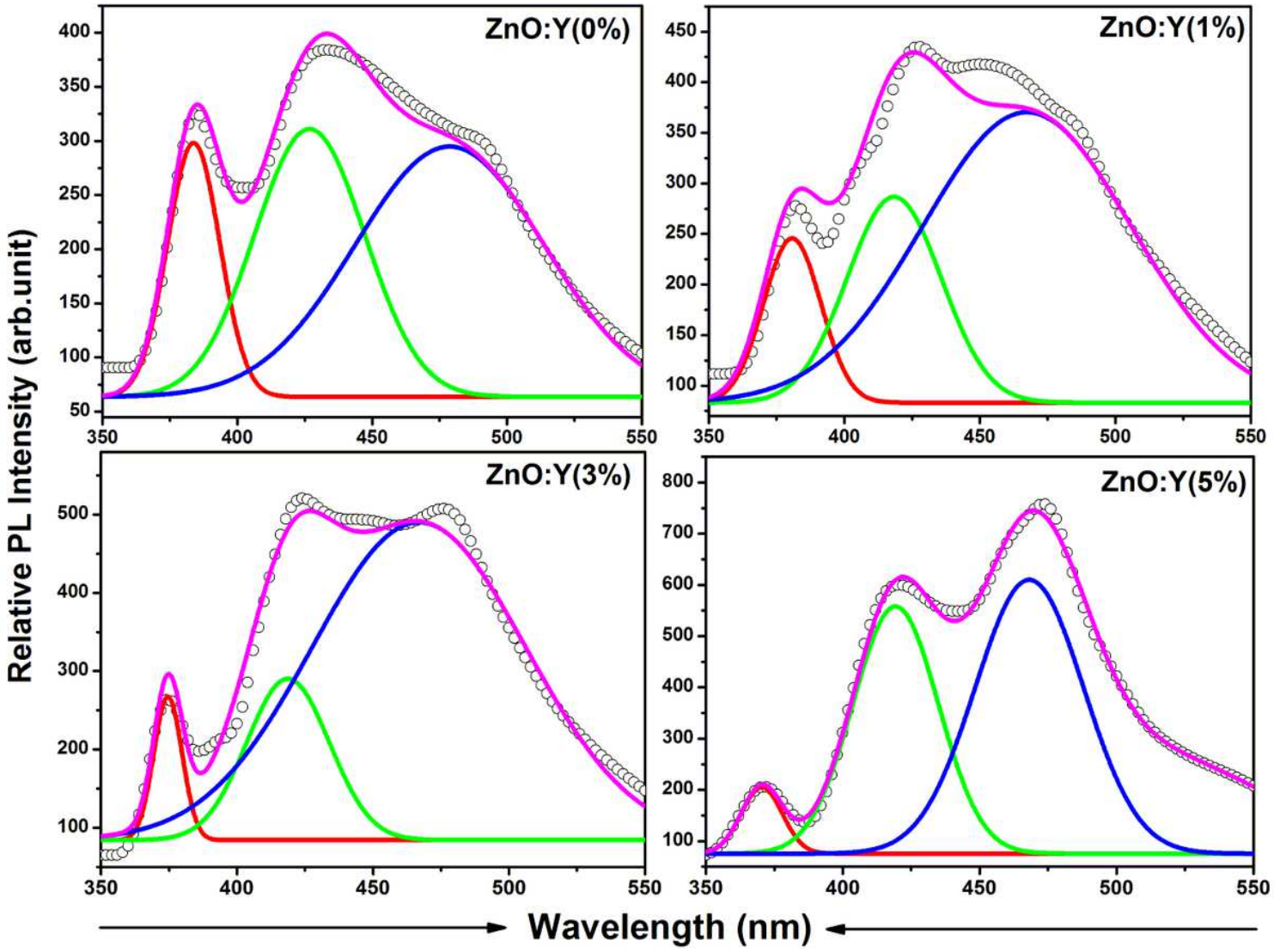

Figure 4

Photoluminescence spectra of ZnO and Y doped ZnO thin films

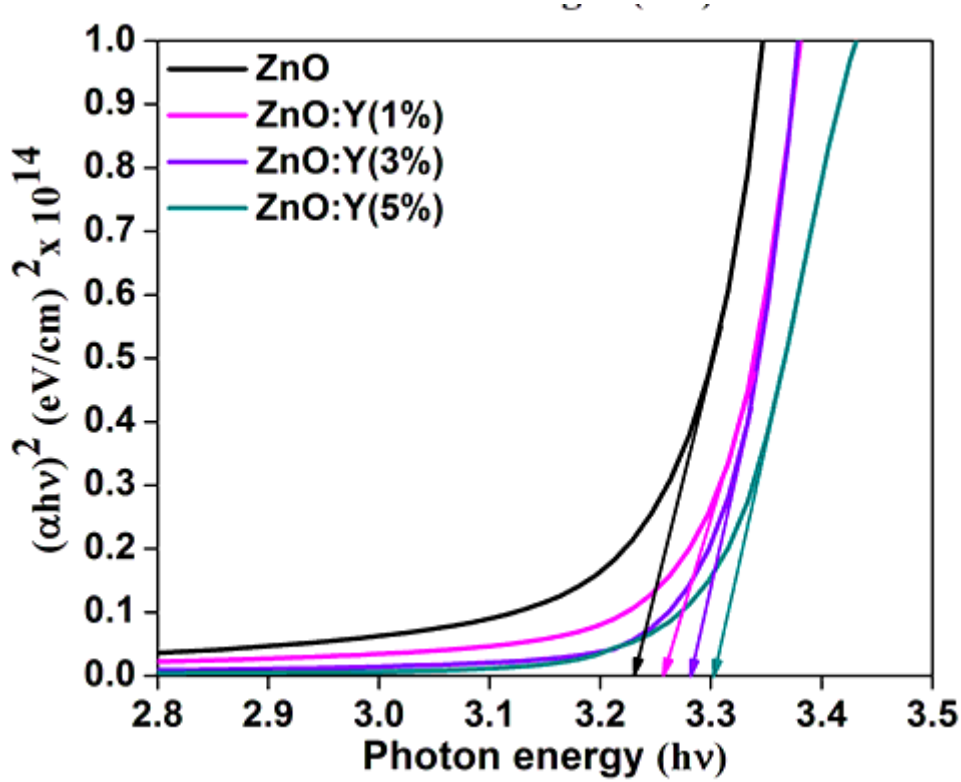

Figure 5

Tauc's plot of ZnO and ZnO:Y (1, 3 and 5 wt%) thin films to measure the bandgap

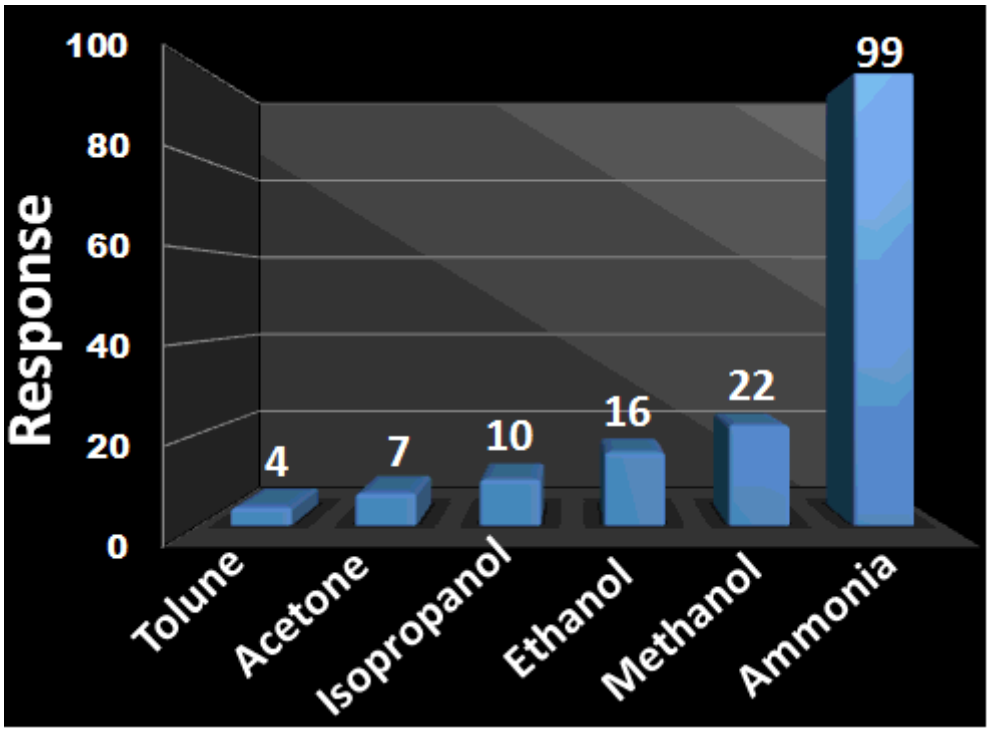

Figure 6

Selectivity of ZnO:Y-5wt% thin film towards various test vapours

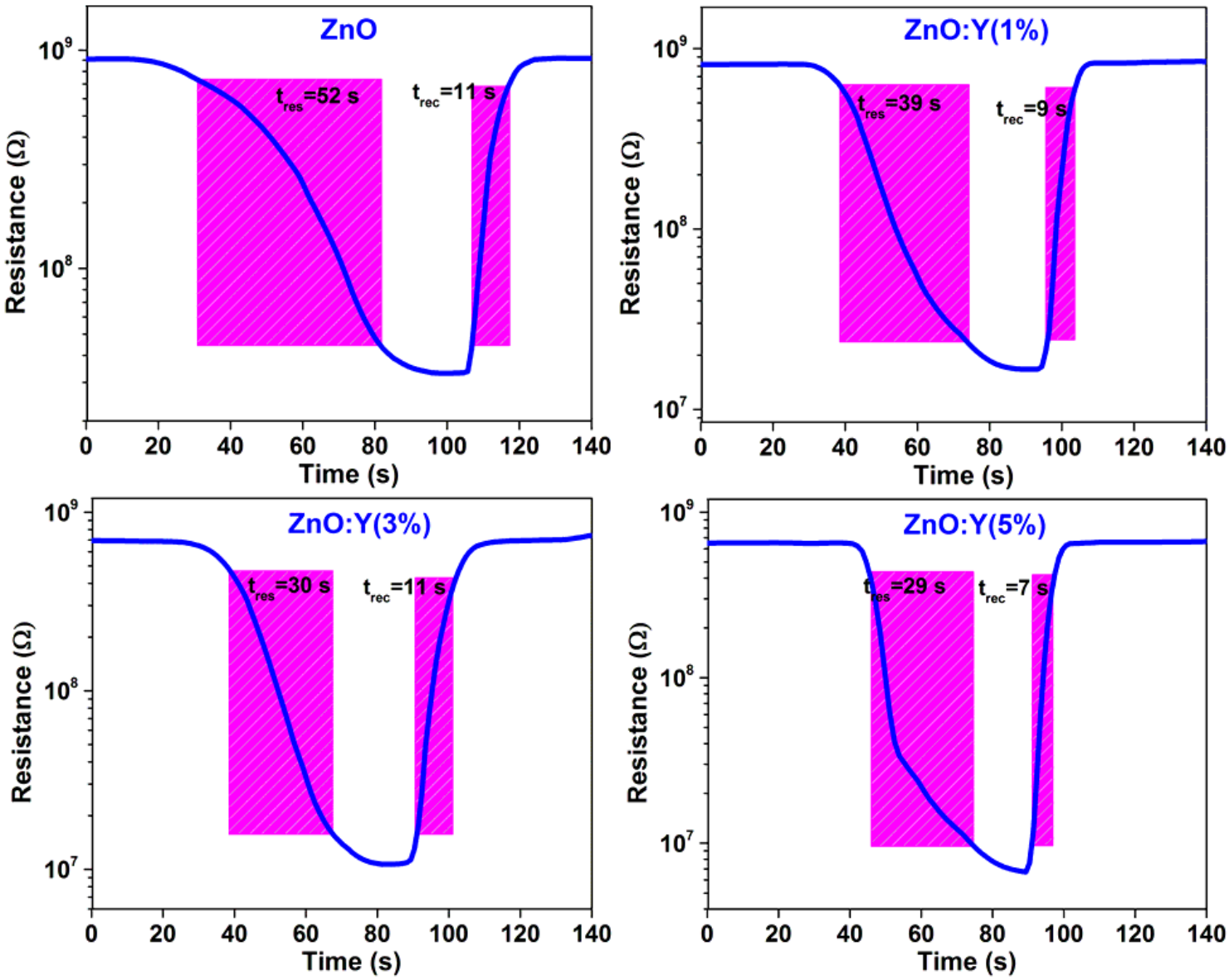

Figure 7

Response and recovery curves of ZnO:Y (0, 1, 3 and 5 wt%) thin films towards 100 ppm of NH3 at room temperature

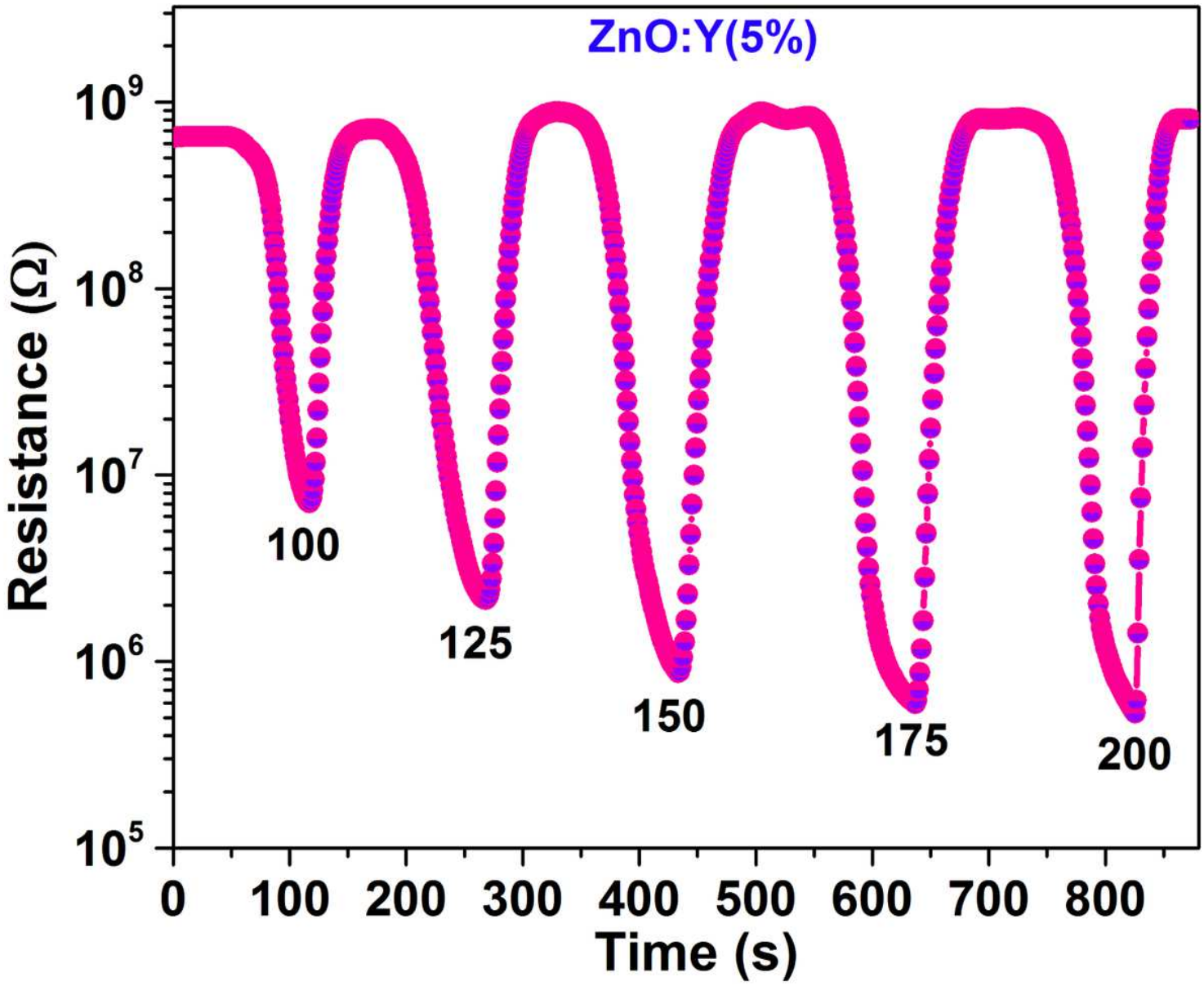

Figure 8

Response and recovery curves of 5 wt% yttrium doped ZnO thin film towards various concentrations of NH3

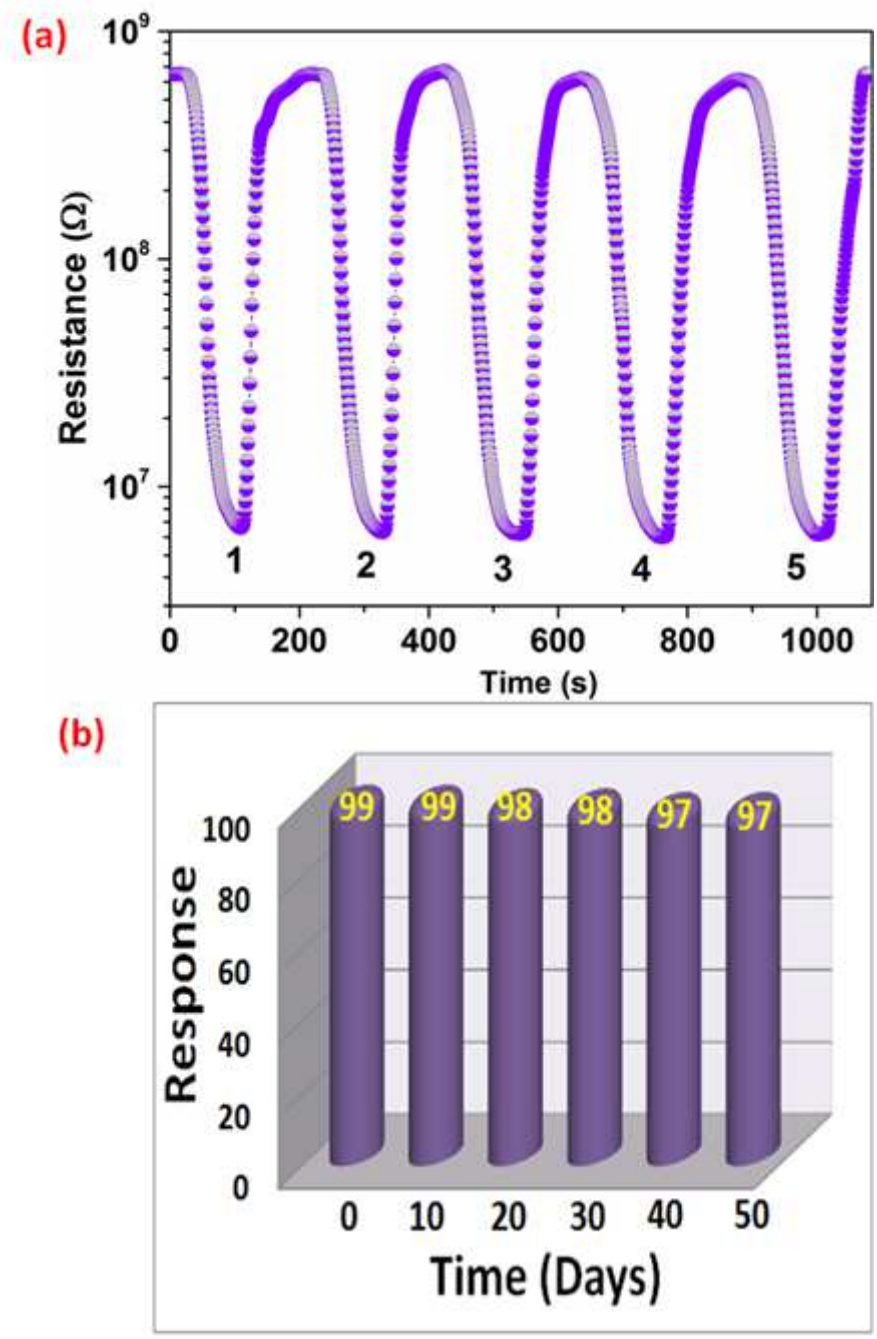

Figure 9

a) Repeatability curve of 5 wt% yttrium doped ZnO thin films b) Stability curve of ZnO:Y (0, 1, 3 and 5 wt%) thin films over 50 days

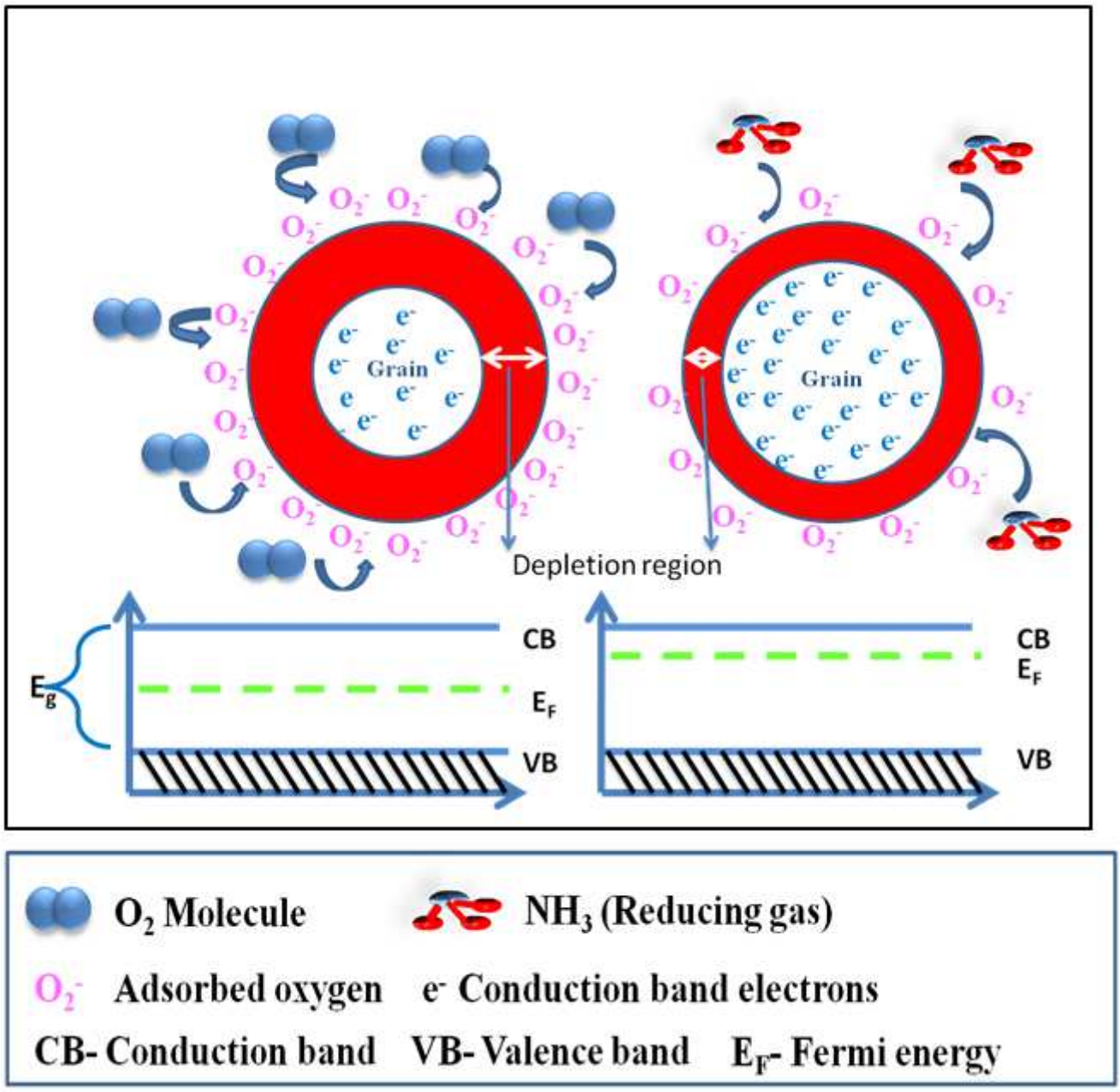

Figure 10

Sensing mechanism of ZnO:Y thin film

Supplementary Files

This is a list of supplementary files associated with this preprint. Click to download.

- Onlinefloatimage10.png